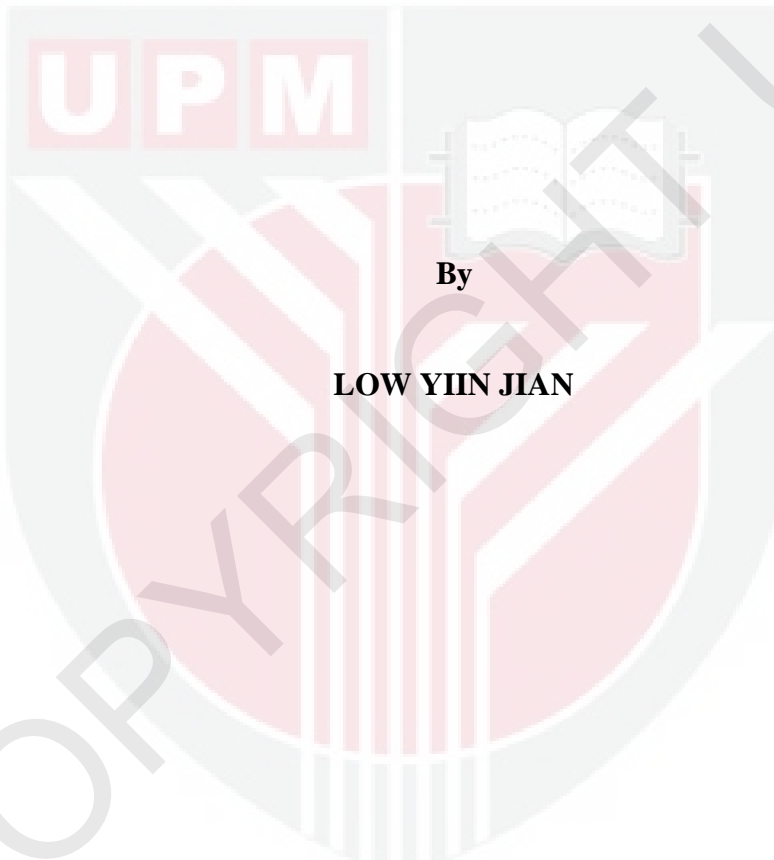




**METHYLAMMONIUM ORGANIC CATION-SUBSTITUTED CESIUM
BISMUTH BROMIDE-BASED PEROVSKITE PREPARED VIA
MICROWAVE-ASSISTED SOLVOTHERMAL METHOD FOR
PHOTOVOLTAIC APPLICATION**



**Thesis Submitted to the School of Graduate Studies, Universiti Putra Malaysia,
in Fulfilment of the Requirements for the Degree of Doctor of Philosophy**

May 2024

ITMA 2024 4

All material contained within the thesis, including without limitation text, logos, icons, photographs and all other artwork, is copyright material of Universiti Putra Malaysia unless otherwise stated. Use may be made of any material contained within the thesis for non-commercial purposes from the copyright holder. Commercial use of material may only be made with the express, prior, written permission of Universiti Putra Malaysia.

Copyright © Universiti Putra Malaysia



Abstract of thesis presented to the Senate of Universiti Putra Malaysia in fulfilment
of the requirement for the degree of Doctor of Philosophy

**METHYLAMMONIUM ORGANIC CATION-SUBSTITUTED CESIUM
BISMUTH BROMIDE-BASED PEROVSKITE PREPARED VIA
MICROWAVE-ASSISTED SOLVOTHERMAL METHOD FOR
PHOTOVOLTAIC APPLICATION**

By

LOW YIIN JIAN

May 2024

Chairman : Josephine Liew Ying Chyi, PhD

Institute : Nanoscience and nanotechnology

Improving Cs-Bi-Br-based perovskites for optoelectronic applications necessitates fast synthesis and thorough investigation of A-site elements. This thesis focuses on the optimization of a microwave-assisted solvothermal method which offers a rapid synthesis for single ($\text{Cs}_3\text{Bi}_2\text{Br}_9$) and double perovskite ($\text{Cs}_2\text{AgBiBr}_6$) materials. The microwave-assisted solvothermal method was optimized with solvent (isopropanol, hexane), ligand (oleic acid, oleylamine) and additive (hydrobromic acid) based on the Cs-Bi-Br-based perovskite materials. The structural and optical characteristics of the synthesized materials were investigated extensively for a better understanding on the material's properties. The research also explores the substitution effect of methylammonium organic cation (MA^+) on the material's properties of single perovskite ($\text{Cs}_{3-x}\text{MA}_x\text{Bi}_2\text{Br}_9$) and double perovskite ($\text{Cs}_{2-x}\text{MA}_x\text{AgBiBr}_6$). A phase segregation event happens in $\text{Cs}_{3-x}\text{MA}_x\text{Bi}_2\text{Br}_9$ when $x \geq 1.0$, causing the formation of $\text{Cs}_3\text{Bi}_2\text{Br}_9$ and $\text{MA}_3\text{Bi}_2\text{Br}_9$ structure with intermediate diffraction plane. Excess of MA^+ substitution in $\text{Cs}_{3-x}\text{MA}_x\text{Bi}_2\text{Br}_9$ reduces the ligands passivation effect and

induced a polydisperse morphology. No significant changes were found in absorption bandgap, Urbach energy and exciton binding energy as MA^+ substitution progress in $\text{Cs}_{3-x}\text{MA}_x\text{Bi}_2\text{Br}_9$. The passivation in non-radiative recombination induced by the intermediate phase formation enhanced the emission intensity and carrier lifetime. Specific thermal decomposition pathway in $\text{Cs}_{3-x}\text{MA}_x\text{Bi}_2\text{Br}_9$ was allocated when $x = 0.5$. While, insignificant amount of MA^+ substitution ($x = 0.2$) relieves the microstrain in $\text{Cs}_2\text{AgBiBr}_6$ structure, increases the volume and reduces the crystallite size without triggering the silver bromide impurities formation. MA^+ also induces defect in structure, causing an aggregation event happens in $\text{Cs}_2\text{AgBiBr}_6$. As the MA^+ substitution increased in $\text{Cs}_{2-x}\text{MA}_x\text{AgBiBr}_6$, the structural disorderment effect caused the absorption energy bandgap red-shifted, Urbach energy rose, and emission intensity reduced. Proper MA^+ substitution ($x = 0.6$) in $\text{Cs}_{2-x}\text{MA}_x\text{AgBiBr}_6$ enhanced the carrier lifetime, but came at the expense of generating a high density of non-radiative recombination. The thermal stability of the $\text{Cs}_{2-x}\text{MA}_x\text{AgBiBr}_6$ is minimally impacted by MA^+ substitution, as the allowed level of MA^+ substitution is limited. Photovoltaic performance of pure $\text{Cs}_2\text{AgBiBr}_6$ surpasses the other materials with a power conversion efficiency of 0.019 %. This research contributes fundamental insights into the investigation of pristine and MA^+ -substituted Cs-Bi-Br based perovskite materials for future photovoltaic applications.

Keywords: Cs-Bi-Br-based perovskites, $\text{Cs}_2\text{AgBiBr}_6$, $\text{Cs}_3\text{Bi}_2\text{Br}_9$, Methylammonium substitution, Microwave-assisted solvothermal synthesis.

SDG: GOAL 7: Affordable and clean energy

Abstrak tesis yang dikemukakan kepada Senat Universiti Putra Malaysia sebagai
memenuhi keperluan untuk ijazah Doktor Falsafah

**PENGGANTIAN KATION ORGANIK METILAMMONIUM DALAM
PEROVSKIT BERASAS CESIUM BISMUTH BROMIDA MELALUI
KAEDAH SOLVOTHERMA BERBANTU MIKROGELOMBANG UNTUK
APLIKASI PHOTOVOLTAIC**

Oleh

LOW YIIN JIAN

Mei 2024

Pengerusi : Josephine Liew Ying Chyi, PhD
Institut : Nanosains dan Nanoteknologi

Penambahbaikan perovskit berasas Cs-Bi-Br untuk aplikasi optoelektronik memerlukan sintesis pantas dan kajian terhadap elemen tapak A. Tesis ini memberi tumpuan kepada pengoptimuman kaedah solvoterma berbantu mikrogelombang yang menawarkan sintesis pantas untuk bahan perovskit tunggal ($Cs_3Bi_2Br_9$) dan perovskit berganda ($Cs_2AgBiBr_6$). Kaedah solvoterma berbantu mikrogelombang telah dioptimumkan dengan pelarut (isopropanol, heksana), ligan (asid oleik, oleamine) dan bahan tambah (asid hidrobromik) berdasarkan bahan perovskite berasas Cs-Bi-Br. Ciri-ciri struktur dan optik bahan yang disintesis telah dikaji secara meluas untuk pemahaman yang lebih baik tentang sifat bahan. Penyelidikan ini juga meninjau kesan penggantian kation organik metilammonium (MA^+) pada sifat bahan perovskite tunggal ($Cs_{3-x}MA_xBi_2Br_9$) dan perovskite berganda ($Cs_{2-x}MA_xAgBiBr_6$). Pengasingan fasa berlaku dalam $Cs_{3-x}MA_xBi_2Br_9$ apabila $x \geq 1.0$, menyebabkan pembentukan struktur $Cs_3Bi_2Br_9$ dan $MA_3Bi_2Br_9$ dengan satah pembelauan perantaraan. Penggantian MA^+ berlebihan dalam $Cs_{3-x}MA_xBi_2Br_9$ mengurangkan kesan pempasifan ligan dan

mendorong morfologi polidispersi. Tiada perubahan ketara didapati dalam jurang jalur serapan, tenaga Urbach dan tenaga ikatan eksiton semasa penambahan penggantian MA^+ dalam $\text{Cs}_{3-x}\text{MA}_x\text{Bi}_2\text{Br}_9$. Pempasifan dalam gabungan semula bukan sinaran yang disebabkan oleh pembentukan fasa perantaraan meningkatkan keamatan pancaran dan jangka hayat pembawa. Laluan penguraian terma khas dalam $\text{Cs}_{3-x}\text{MA}_x\text{Bi}_2\text{Br}_9$ diperuntukkan apabila $x = 0.5$. Manakala, jumlah penggantian MA^+ yang tidak ketara ($x = 0.2$) melegakan mikroterikan dalam struktur $\text{Cs}_2\text{AgBiBr}_6$, meningkatkan isipadu dan mengurangkan saiz kristalit tanpa mencetuskan pembentukan bendasing argentum bromida. MA^+ juga mendorong kecacatan dalam struktur, menyebabkan pengagregatan berlaku dalam $\text{Cs}_2\text{AgBiBr}_6$. Apabila penggantian MA^+ meningkat dalam $\text{Cs}_{2-x}\text{MA}_x\text{AgBiBr}_6$, kesan struktur tak tertib menyebabkan tenaga jurang jalur serapan beralih merah, tenaga Urbach meningkat dan keamatan pancaran berkurangan. Penggantian MA^+ yang sesuai ($x = 0.6$) dalam $\text{Cs}_{2-x}\text{MA}_x\text{AgBiBr}_6$ meningkatkan jangka hayat pembawa, tetapi mendatangkan penjanaan ketumpatan gabungan semula bukan sinaran yang tinggi. Kestabilan terma $\text{Cs}_{2-x}\text{MA}_x\text{AgBiBr}_6$ dipengaruhi secara minimum oleh penggantian MA^+ , disebabkan tahap penggantian MA^+ yang dibenarkan adalah terhad. Prestasi fotovolta $\text{Cs}_2\text{AgBiBr}_6$ tulen melepas bahan lain dengan kecekapan penukaran kuasa sebanyak 0.019 %. Penyelidikan ini menyumbang wawasan asas dalam kajian bahan perovskit berasas Cs-Bi-Br yang murni dan digantikan oleh MA^+ untuk aplikasi fotovolta masa hadapan.

Kata Kunci: Perovskit berasas Cs-Bi-Br, $\text{Cs}_2\text{AgBiBr}_6$, $\text{Cs}_3\text{Bi}_2\text{Br}_9$, Penggantian metilammonium, Kaedah solvotherma berbantu mikrogelombang

SDG: MATLAMAT 7: Tenaga Berpatutan dan Bersih

ACKNOWLEDGEMENTS

I'm deeply grateful to those who have played crucial roles in my journey:

Firstly, my heartfelt thanks to my family for their unwavering moral and financial support. Their constant belief in my abilities has been pivotal to my success.

A special appreciation goes to my supervisor, Dr. Josephine, for her invaluable guidance, encouragement, and financial support during my Ph.D. Her expertise shaped my research and motivated me to excel.

I extend my gratitude to my supervisory committee: Prof. Janet Lim Hong Ngee, Assoc. Prof. Dr. Lim Kean Pah, Dr. Mohd Hafiz Mohd Zaid, and Dr. Choo Thye Foo, for their continual moral support and guidance.

My appreciation extends to the Malaysian Nuclear Agency (ANM) for their invaluable collaboration and resources in material characterization, enriching my research.

I acknowledge RGS Cooperation for the opportunities and financial aid during my tenure, broadening my knowledge and skills. Prof. Han Sang-Wook from Jeonbuk National University is also thanked for providing the chance to conduct XAFS measurements in PLS-II.

Dr. Mazliana Ahmad Kamarudin's generosity in providing the Monowave 300 was indispensable for my project's success. Her support was pivotal in achieving my project's objectives.

Lastly, I thank Dr. Farah Diana Muhammad and Dr. Chan Kar Tim for their grant support and opportunities in exploring diverse areas of materials research. Their belief in my potential has shaped my research direction.

To each of you, your unwavering support, encouragement, and contributions have been invaluable. Working with exceptional individuals and organizations like you has been an honor. My heartfelt gratitude for your contributions to my success.

This thesis was submitted to the Senate of Universiti Putra Malaysia and has been accepted as fulfilment of the requirement for the degree of Doctor of Philosophy. The members of the Supervisory Committee were as follows:

Josephine Liew Ying Chyi, PhD

Senior Lecturer

Faculty of Science

Universiti Putra Malaysia

(Chairman)

Janet Lim Hong Ngee, PhD

Professor ChM.

Faculty of Science

Universiti Putra Malaysia

(Member)

Lim Kean Pah, PhD

Associate Professor

Faculty of Science

Universiti Putra Malaysia

(Member)

Mohd Hafiz bin Mohd Zaid, PhD

Senior Lecturer

Faculty of Science

Universiti Putra Malaysia

(Member)

Choo Thye Foo, PhD

Research Officer

Materials Technology Group

Agensi Nuklear Malaysia

(Member)

ZALILAH MOHD SHARIFF, PhD

Professor and Dean

School of Graduate Studies

Universiti Putra Malaysia

Date: 8 August 2024

TABLE OF CONTENTS

	Page
ABSTRACT	i
ABSTRAK	iii
ACKNOWLEDGEMENTS	v
APPROVAL	vii
DECLARATION	ix
LIST OF TABLES	xiv
LIST OF FIGURES	xvi
LIST OF ABBREVIATIONS	xxii
 CHAPTER	
1 INTRODUCTION	1
1.1 Overview of bismuth-based perovskite halides	1
1.2 Problem statement	3
1.3 Hypotheses	4
1.4 Objectives	6
1.5 Scope of study	6
1.6 Thesis outline	7
2 LITERATURE REVIEW	8
2.1 Synthesis methods for Cs-Bi-Br-based perovskite materials	8
2.1.1 Microwave-assisted solvothermal method	8
2.1.2 Hot-injection method	14
2.1.3 Re-precipitation method	21
2.2 Cs-Bi-Br-based perovskite materials	26
2.2.1 Material's properties and bandgap engineering of $Cs_3Bi_2Br_9$	26
2.2.2 Material's properties and bandgap engineering of $Cs_2AgBiBr_6$	53
2.3 Opportunities of the mixed organic/inorganic A-site cation system in other high performance perovskite structure	91
2.4 Summary of the synthesis methods, materials properties, bandgap engineering and photovoltaic application of Cs-Bi-Br-based perovskites	97
3 METHODOLOGY	101
3.1 Synthesis of the precursors for Cs-Bi-Br-based perovskite materials	101
3.6.1 Methylammonium bromide	101
3.6.2 Silver bromide	102
3.2 Synthesis of Cs-Bi-Br-based perovskite materials	103
3.3 Synthesis of Cs-Bi-Br-based perovskite materials with methylammonium bromide	112

3.4	Material characterization	116
3.4.1	X-ray diffraction	116
3.4.2	Raman spectroscopy	121
3.4.3	X-ray absorption fine structure spectroscopy	122
3.4.4	Field-emission scanning electron microscopy	128
3.4.5	Energy dispersive x-ray spectroscopy	130
3.4.6	Thermogravimetric analysis	131
3.4.7	Ultraviolet-visible diffuse reflectance spectroscopy	132
3.4.8	Photoluminescence spectroscopy	135
3.4.9	Temperature-dependent photoluminescence spectroscopy	136
3.4.10	Time-resolved photoluminescence spectroscopy	139
3.5	Photovoltaic performance evaluation	141
	Cs-Bi-Br-based perovskite device fabrication	141
	Current-voltage measurement	143
3.6	Error estimation in measurement and analysis	145
4	RESULTS AND DISCUSSION	147
4.1	Synthesis of perovskite precursor	147
4.1.1	Methylammonium bromide precursor	147
4.1.2	Silver bromide precursor	149
4.2	Optimization of the synthesis of $\text{Cs}_3\text{Bi}_2\text{Br}_9$	150
4.3	Material properties of the synthesized $\text{Cs}_3\text{Bi}_2\text{Br}_9$	154
4.3.1	Structural properties	154
4.3.2	Morphological properties	157
4.3.3	Elemental properties	159
4.3.4	Optical properties	160
4.3.5	Thermal stability	166
4.3.6	Comparing microwave-assisted solvothermal method with other methods for Cs-Bi-Br-based single perovskites	168
4.4	Optimization of the synthesis of $\text{Cs}_2\text{AgBiBr}_6$	171
4.5	Material properties of the synthesized $\text{Cs}_2\text{AgBiBr}_6$	176
4.5.1	Structural properties	176
4.5.2	Morphological properties	179
4.5.3	Elemental properties	181
4.5.4	Optical properties	182
4.5.5	Thermal stability	192
4.5.6	Comparing microwave-assisted solvothermal method with other methods for $\text{Cs}_2\text{AgBiBr}_6$	194

4.6	Comparison of the material properties between single and double Cs-Bi-Br-based perovskite	197
4.7	MA ⁺ substitution effect in Cs ₃ Bi ₂ Br ₉	199
4.7.1	Structural properties	199
4.7.2	Morphological properties	207
4.7.3	Elemental properties	209
4.7.4	Optical properties	210
4.7.5	Thermal stability	221
4.8	MA ⁺ substitution effect in Cs ₂ AgBiBr ₆	225
4.8.1	Structural properties	225
4.8.2	Morphological properties	240
4.8.3	Elemental properties	242
4.8.4	Optical properties	243
4.8.5	Thermal stability	254
4.9	Comparison of the MA ⁺ substitution effect in single and double Cs-Bi-Br-based perovskite	260
4.10	Photovoltaic performance of Cs-Bi-Br-based perovskite materials	263
4.10.1	Photovoltaic performance of MA ⁺ -substituted Cs ₃ Bi ₂ Br ₉ materials	263
4.10.2	Photovoltaic performance of MA ⁺ -substituted Cs ₂ AgBiBr ₆ materials	265
5	CONCLUSION AND FUTURE WORK	267
5.1	Conclusion	267
5.2	Future perspective	271
REFERENCES		272
APPENDICES		297
BIODATA OF STUDENT		299
LIST OF PUBLICATIONS		301

LIST OF TABLES

Table		Page
2.1	Summary of the microwave-assisted solvothermal method synthesis details and the resulting perovskite materials properties.	12
2.2	Summary of the HIM synthesis details of and the resulting Cs-Bi-Br-based perovskite materials properties.	15
2.3	Summary of the RM synthesis details of and the resulting Cs-Bi-Br-based perovskite materials properties.	23
2.4	Summary of the morphology and optical properties of $\text{Cs}_3\text{Bi}_2\text{Br}_9$.	30
2.5	Summary of the substitutes in the A-site of $\text{Cs}_3\text{Bi}_2\text{Br}_9$.	36
2.6	Summary of the substitutes in the B-site of $\text{Cs}_3\text{Bi}_2\text{Br}_9$.	39
2.7	Summary of the substitutes in the X-site of $\text{Cs}_3\text{Bi}_2\text{Br}_9$.	46
2.8	Summary of the morphology and optical properties of $\text{Cs}_2\text{AgBiBr}_6$.	57
2.9	Summary of the substitutes in the A-site of $\text{Cs}_2\text{AgBiBr}_6$.	70
2.10	Summary of the substitutes in the B^{I} -site of $\text{Cs}_2\text{AgBiBr}_6$.	74
2.11	Summary of the substitutes in the B^{III} -site of $\text{Cs}_2\text{AgBiBr}_6$.	77
2.12	Summary of the substitutes in the mixed $\text{B}^{\text{I}}/\text{B}^{\text{III}}$ -site $\text{Cs}_2\text{AgBiBr}_6$.	83
2.13	Summary of the substitutes in the X-site of $\text{Cs}_2\text{AgBiBr}_6$.	86
2.14	Summary of the structural and optical properties found in high performance perovskite halide materials subsequent to mixed organic/inorganic A-site cations engineering.	93
3.1	Chemical used in the Cs-Bi-Br-based perovskite synthesis.	104
3.2	Energy edges of chosen elements (Source: Bearden et al., 1967).	123
3.3	Propagation of errors with different relation in mathematical equation.	146
4.1	XRD Rietveld refinement data of the synthesized $\text{Cs}_3\text{Bi}_2\text{Br}_9$.	156
4.2	Chemical composition of the synthesized $\text{Cs}_2\text{AgBiBr}_6$.	159

4.3	Carrier lifetime components and proportion of $\text{Cs}_3\text{Bi}_2\text{Br}_9$.	165
4.4	Summary of the $\text{Cs}_3\text{Bi}_2\text{Br}_9$ synthesized with different methods and its properties	170
4.5	XRD Rietveld refinement data of the synthesized $\text{Cs}_2\text{AgBiBr}_6$.	178
4.6	Chemical composition of $\text{Cs}_2\text{AgBiBr}_6$.	182
4.7	Parameters of the relevant equations after being fitted to the TDPL data.	190
4.8	Carrier lifetime components and proportion of $\text{Cs}_2\text{AgBiBr}_6$.	192
4.9	Summary of the synthesis methods and properties of $\text{Cs}_2\text{AgBiBr}_6$.	196
4.10	Rietveld quantitative XRD phase analysis of $\text{Cs}_{3-x}\text{MA}_x\text{Bi}_2\text{Br}_9$.	204
4.11	Raman peak properties of $\text{Cs}_{3-x}\text{MA}_x\text{Bi}_2\text{Br}_9$ revealed after the deconvolution process.	207
4.12	Chemical compositions of $\text{Cs}_{3-x}\text{MA}_x\text{Bi}_2\text{Br}_9$.	209
4.13	Carrier lifetime components of $\text{Cs}_{3-x}\text{MA}_x\text{Bi}_2\text{Br}_9$ with varied MA^+ substitution composition.	220
4.14	Rietveld quantitative XRD phase analysis and Williamson-Hall plot of $\text{Cs}_{2-x}\text{MA}_x\text{AgBiBr}_6$.	229
4.15	Raman peak properties of $\text{Cs}_{2-x}\text{MA}_x\text{AgBiBr}_6$ revealed after the deconvolution process.	234
4.16	Chemical compositions of $\text{Cs}_{2-x}\text{MA}_x\text{AgBiBr}_6$.	242
4.17	Carrier lifetime components of $\text{Cs}_{2-x}\text{MA}_x\text{AgBiBr}_6$ with varied MA^+ substitution composition.	252

LIST OF FIGURES

Figure		Page
2.1	Mechanism of (a) ionic conduction and (b) dipolar polarization; temperature gradient of (c) microwave-assisted solvothermal method and (d) conventional solvothermal method. (Source: Kunal et al., 2020)	10
2.2	Schematic illustration of the experimental setup and procedure for the hot-injection method. (Source: Shamsi et al., 2019)	14
2.3	Schematic illustration of the experimental setup and procedure for the re-precipitation method. (Source: Shamsi et al., 2019)	22
2.4	Unit cell of $\text{Cs}_3\text{Bi}_2\text{Br}_9$. (Source: Geng et al., 2021)	27
2.5	The arrangement of $\text{Cs}_3\text{Bi}_2\text{Br}_9$ structure as viewed from (a) a parallel perspective to the Bi-Br octahedron, (b) a direct viewpoint along the Bi-Br bonding, and (c) a rotated perspective of Bi-Br bonding. (Source: Shi et al., 2020)	27
2.6	(a) Electronic band structure and, (b) density of state of $\text{Cs}_3\text{Bi}_2\text{Br}_9$. (Source: Wang et al., 2021a)	29
2.7	Unit cell of $\text{Cs}_2\text{AgBiBr}_6$. (Source: Yang et al., 2018c)	53
2.8	The arrangement of $\text{Cs}_2\text{AgBiBr}_6$ structure observed from (a) parallel perspective, (b) direct viewpoint and (c) rotated perspective of the Bi-Br and Ag-Br bonding. (Source: Shi et al., 2020)	54
2.9	(a) Electronic band structure and (b) density of state of $\text{Cs}_2\text{AgBiBr}_6$. (Source: Xiao et al., 2016)	56
3.1	The experimental procedure for the Cs-Bi-Br-based perovskite prepared via the microwave-assisted solvothermal method.	103
3.2	The flowchart detailing the optimization procedure for synthesizing $\text{Cs}_3\text{Bi}_2\text{Br}_9$.	106
3.3	The flowchart detailing the optimization procedure for synthesizing $\text{Cs}_2\text{AgBiBr}_6$.	108
3.4	Synthesis process of pure $\text{Cs}_3\text{Bi}_2\text{Br}_9$.	110
3.5	Synthesis process of pure $\text{Cs}_2\text{AgBiBr}_6$.	111

3.6	Synthesis process of MA^+ -substituted $\text{Cs}_3\text{Bi}_2\text{Br}_9$.	114
3.7	Synthesis process of MA^+ -substituted $\text{Cs}_2\text{AgBiBr}_6$.	115
3.8	Schematic illustration of Bragg's diffraction. (Source: Leng, 2010)	117
3.9	Instrument setup for XRD under Bragg-Brentano geometry. (Source: König et al., 2012)	118
3.10	The structure of $\text{Cs}_2\text{AgBiBr}_6$. (Source: Burwig et al., 2020)	124
3.11	Experimental setup of XAFS in transmission mode and fluorescence mode. (Source: Wu et al., 2021c)	125
3.12	Schematic illustration for FESEM setup. (Source: Che Hak et al., 2015)	129
3.13	Schematic illustration of PL spectroscopy setup (Source: Fernández-Castillejo et al., 2022).	136
3.14	Schematic illustration of TCSPC technique in TRPL measurement (Source: Harrison, 2016)	140
3.15	Solar cell device structure used for performance evaluation.	142
3.16	I-V calibration curve using commercial solar cell.	144
4.1	XRD patterns for the (a) sample holder, (b) MABr database, (c) MABr under spinning and (d) MABr without spinning.	148
4.2	XRD patterns for the synthesized AgBr compared to AgBr database.	149
4.3	XRD patterns of sample synthesized using (a) ODE and (b) IPA/hexane as solvents.	151
4.4	(a) XRD pattern for different OA : OLA ratio with constant HBr amount and (b) optimized OA : OLA ratio with different HBr amount in binary IPA/hexane solvent system.	153
4.5	$\text{Cs}_3\text{Bi}_2\text{Br}_9$ XRD patterns obtained from experimental and database.	155
4.6	Lattice structure of $\text{Cs}_3\text{Bi}_2\text{Br}_9$.	155
4.7	Raman spectrum of the synthesized $\text{Cs}_3\text{Bi}_2\text{Br}_9$.	157
4.8	FESEM images of the synthesized $\text{Cs}_3\text{Bi}_2\text{Br}_9$ at (a) x5K, (b) x10K magnifications, and (c) calculated lateral size distribution histogram.	158

4.9	EDX spectrum of the synthesized $\text{Cs}_2\text{AgBiBr}_6$.	159
4.10	(a) Absorption spectrum, (b) Elliot model fitting, (c) direct allowed transition Tauc plot, and (d) Urbach fitting of the synthesized $\text{Cs}_3\text{Bi}_2\text{Br}_9$.	162
4.11	(a) Temperature-dependent photoluminescence spectra, (b) peak energies, (c) peak intensities and (d) peak intensity ratio measured from 77 K – 300 K.	164
4.12	Time-resolved photoluminescence of synthesized $\text{Cs}_3\text{Bi}_2\text{Br}_9$ fitted with tri-exponential tail fit equation (red line).	165
4.13	Thermogravimetric analyses of the synthesized $\text{Cs}_3\text{Bi}_2\text{Br}_9$.	168
4.14	XRD patterns of materials formed in (a) ODE and (b) IPA solvents.	172
4.15	XRD pattern of materials formed under (a) 1.5 ml (b) 2.0 ml and (c) 2.5 ml of HBr with different OA : OLA ratio in IPA solvent.	175
4.16	Database and experimental XRD pattern of the synthesized $\text{Cs}_2\text{AgBiBr}_6$.	177
4.17	Lattice structure of $\text{Cs}_2\text{AgBiBr}_6$.	177
4.18	Raman spectrum of $\text{Cs}_2\text{AgBiBr}_6$.	179
4.19	FESEM images of $\text{Cs}_2\text{AgBiBr}_6$ under (a) x20k and (b) x50k magnification and (c) calculated lateral size distribution histogram.	180
4.20	EDX spectrum of $\text{Cs}_2\text{AgBiBr}_6$.	181
4.21	Absorption spectrum of $\text{Cs}_2\text{AgBiBr}_6$.	183
4.22	(a) Indirect and (b) direct allowed transitions of $\text{Cs}_2\text{AgBiBr}_6$.	183
4.23	Band-to-band transitions of $\text{Cs}_2\text{AgBiBr}_6$.	183
4.24	Absorption tail of $\text{Cs}_2\text{AgBiBr}_6$ fitted with Urbach equation.	184
4.25	Temperature-dependance photoluminescence spectra of $\text{Cs}_2\text{AgBiBr}_6$ within 77 K - 300 K.	185
4.26	(a) Radiative recombination (b) non-radiative recombination originated from scattered-direct exciton and (c) indirect exciton in $\text{Cs}_2\text{AgBiBr}_6$.	186
4.27	Peak energies of TDPL measured in the temperature range of 77 K – 300 K with the fitting of the Varshni equation.	187

4.28	Peak intensities of TDPL measured in the temperature range of 77 K – 300 K with the fitting of the Arrhenius equation.	189
4.29	FWHM of TDPL measured in the temperature range of 77 K – 300 K with the fitting of the Boson equation.	190
4.30	Time-resolved photoluminescence spectrum of $\text{Cs}_2\text{AgBiBr}_6$ with tri-exponential tail fitting (red line).	191
4.31	Thermogravimetric analyses and derivative thermogravimetric of the synthesized $\text{Cs}_2\text{AgBiBr}_6$.	193
4.32	(a) Full scale and (b) focused XRD patterns of synthesized $\text{Cs}_{3-x}\text{MA}_x\text{Bi}_2\text{Br}_9$ (b) with the (022) plane peak position.	201
4.33	Physical appearance of $\text{Cs}_{3-x}\text{MA}_x\text{Bi}_2\text{Br}_9$ as MA^+ composition increases.	202
4.34	(a) Phase composition, (b) lattice parameters and (c) volume of the synthesized $\text{Cs}_{3-x}\text{MA}_x\text{Bi}_2\text{Br}_9$ as MA^+ composition progress.	203
4.35	Raman spectra of $\text{Cs}_{3-x}\text{MA}_x\text{Bi}_2\text{Br}_9$.	206
4.36	Bond length of Bi-Br octahedra accessed from $\text{Cs}_3\text{Bi}_2\text{Br}_9$ and $\text{MA}_3\text{Bi}_2\text{Br}_9$ database view from c-direction.	206
4.37	FESEM images and lateral size distributions of $\text{Cs}_{3-x}\text{MA}_x\text{Bi}_2\text{Br}_9$ when (a-b) $x = 0$, (c-d) 1.0, (e-f) 2.0.	208
4.38	Chemical composition and XRD-derived phase composition of $\text{Cs}_{3-x}\text{MA}_x\text{Bi}_2\text{Br}_9$.	210
4.39	Absorbance spectra of $\text{Cs}_{3-x}\text{MA}_x\text{Bi}_2\text{Br}_9$.	211
4.40	Direct energy bandgap of $\text{Cs}_{3-x}\text{MA}_x\text{Bi}_2\text{Br}_9$ determined from Tauc equation for (a) $x = 0$, (b) 0.5, (c) 1.0, (d) 1.5, (e) 2.0 and (f) 2.5, respectively.	212
4.41	Direct energy bandgap of $\text{Cs}_{3-x}\text{MA}_x\text{Bi}_2\text{Br}_9$.	213
4.42	Exciton binding energy of $\text{Cs}_{3-x}\text{MA}_x\text{Bi}_2\text{Br}_9$ derived from Elliot equation for (a) $x = 0$, (b) 0.5, (c) 1.0, (d) 1.5, (e) 2.0 and (f) 2.5, respectively.	214
4.43	Exciton binding energy determined from Elliot fitting of $\text{Cs}_{3-x}\text{MA}_x\text{Bi}_2\text{Br}_9$.	215
4.44	Urbach-fitted absorbance graph of $\text{Cs}_{3-x}\text{MA}_x\text{Bi}_2\text{Br}_9$ for (a) $x = 0$, (b) 0.5, (c) 1.0, (d) 1.2, (e) 2.0 and (f) 2.5.	216
4.45	Urbach energy of $\text{Cs}_{3-x}\text{MA}_x\text{Bi}_2\text{Br}_9$.	217

4.46	(a) Photoluminescence spectra, (b) peak intensities and full-width half maximum (FWHM) at 490 nm of $\text{Cs}_{3-x}\text{MA}_x\text{Bi}_2\text{Br}_9$.	218
4.47	(a) Time-resolved photoluminescence spectra, (b) carrier rate equation fitted curve and (c) the average carrier lifetime of $\text{Cs}_{3-x}\text{MA}_x\text{Bi}_2\text{Br}_9$ with different MA^+ substitution amount.	219
4.48	TGA and DTG of $\text{Cs}_{3-x}\text{MA}_x\text{Bi}_2\text{Br}_9$ for (a) $x = 0$, (b) 0.5, (c) 1.0, (d) 1.5, (e) 2.0 and (f) 2.5, respectively.	222
4.49	(a) TGA and (b) DTG stacking curve of $\text{Cs}_{3-x}\text{MA}_x\text{Bi}_2\text{Br}_9$, with the (c) extracted mass loss as x progressed.	223
4.50	XRD patterns of $\text{Cs}_{2-x}\text{MA}_x\text{AgBiBr}_6$ with different MA^+ compositions.	227
4.51	Physical appearance of $\text{Cs}_{2-x}\text{MA}_x\text{AgBiBr}_6$ as MA^+ composition increases.	227
4.52	Williamson-Hall plot of $\text{Cs}_{2-x}\text{MA}_x\text{AgBiBr}_6$ when (a) $x = 0$, (b) 0.2, (c) 0.4, (d) 0.6, (e) 0.8, and (f) 1.0, respectively.	228
4.53	Microstrain and crystallite size values of $\text{Cs}_{2-x}\text{MA}_x\text{AgBiBr}_6$ as x progress.	230
4.54	Phase compositions of $\text{Cs}_{2-x}\text{MA}_x\text{AgBiBr}_6$ as x progress.	232
4.55	Volume of $\text{Cs}_{2-x}\text{MA}_x\text{AgBiBr}_6$ as x progress.	233
4.56	Raman spectra of $\text{Cs}_{2-x}\text{MA}_x\text{AgBiBr}_6$.	234
4.57	Normalized total X-ray absorption at Bi L ₁ edge in $\text{Cs}_{2-x}\text{MA}_x\text{AgBiBr}_6$ powders as a function of the incident X-ray energy.	235
4.58	EXAFS of Bi L ₁ edge in $\text{Cs}_{2-x}\text{MA}_x\text{AgBiBr}_6$ powders as a function of photoelectron wave number, k .	236
4.59	Fourier-transformed EXAFS of Bi L ₁ edge in $\text{Cs}_{2-x}\text{MA}_x\text{AgBiBr}_6$ powders as a function of the lattice parameter.	237
4.60	Fourier-transformed EXAFS of Bi L ₁ edge in $\text{Cs}_{2-x}\text{MA}_x\text{AgBiBr}_6$ powders as a function of lattice parameter, R with an intention shift in the y-axis.	237

4.61	Theoretical simulation of crystal structures for $\text{Cs}_{2-x}\text{MA}_x\text{AgBiBr}_6$ with nine different compositions. Color-code for atoms: Cs (green), Ag (purple), Bi (gray), Br (brown), C (silver), N (light-brown), H (white) (Source: Wu et al., 2022b).	238
4.62	FESEM images and lateral size distributions of $\text{Cs}_{2-x}\text{MA}_x\text{AgBiBr}_6$ when (a-b) $x = 0$, (c-d) 0.2, (e-f) 0.6, (g-h) 1.0.	241
4.63	Chemical composition and XRD-derived phase composition of $\text{Cs}_{2-x}\text{MA}_x\text{AgBiBr}_6$.	243
4.64	Absorbance spectra of $\text{Cs}_{2-x}\text{MA}_x\text{AgBiBr}_6$.	243
4.65	Direct energy bandgap of $\text{Cs}_{2-x}\text{MA}_x\text{AgBiBr}_6$ determined from Tauc equation for (a) $x = 0$, (b) 0.2, (c) 0.4, (d) 0.6, (e) 0.8 and (f) 1.0.	245
4.66	Indirect energy bandgap of $\text{Cs}_{2-x}\text{MA}_x\text{AgBiBr}_6$ determined from Tauc equation for (a) $x = 0$, (b) 0.2, (c) 0.4, (d) 0.6, (e) 0.8 and (f) 1.0.	246
4.67	Direct and indirect energy bandgap of $\text{Cs}_{2-x}\text{MA}_x\text{AgBiBr}_6$ as x progress.	247
4.68	Urbach-fitted absorbance graph of $\text{Cs}_{2-x}\text{MA}_x\text{AgBiBr}_6$ for (a) $x = 0$, (b) 0.2, (c) 0.4, (d) 0.6, (e) 0.8 and (f) 1.0.	248
4.69	Urbach energy of $\text{Cs}_{2-x}\text{MA}_x\text{AgBiBr}_6$ as x progress.	249
4.70	(a) Photoluminescence spectra, (b) peak intensities and full-width half maximum (FWHM) of $\text{Cs}_{2-x}\text{MA}_x\text{AgBiBr}_6$.	251
4.71	(a) Time-resolved photoluminescence spectra, (b) carrier rate equation fitted curve and (c) the average carrier lifetime of $\text{Cs}_{2-x}\text{MA}_x\text{AgBiBr}_6$ with different MA^+ substitution composition.	252
4.72	TGA and DTG of $\text{Cs}_{2-x}\text{MA}_x\text{AgBiBr}_6$ for (a) $x = 0$, (b) 0.2, (c) 0.4, (d) 0.6, (e) 0.8 and (f) 1.0, respectively.	256
4.73	(a) TGA and (b) DTG stacking curve of $\text{Cs}_{2-x}\text{MA}_x\text{AgBiBr}_6$, with the (c) extracted mass loss as x progressed.	257
4.74	(a) I-V curve, (b) V_{oc} , J_{sc} , (c) FF, and PCE of $\text{Cs}_{3-x}\text{MA}_x\text{Bi}_2\text{Br}_9$.	264
4.75	(a) I-V curve, (b) V_{oc} , J_{sc} , (c) FF, and PCE of $\text{Cs}_{2-x}\text{MA}_x\text{AgBiBr}_6$.	266

LIST OF ABBREVIATIONS

-	A span range of number
~	Approximately
1L	One-layered
2L	Two-layered
2D	Two dimensions
3D	Three dimensions
A-EtOH	Absolute ethanol
ACN	Acetonitrile
Ag(OAc)	Silver acetate
AgBr	Silver bromide
AgNO ₃	Silver nitrate
ANM	Malaysian Nuclear Agency
Bi(OAc) ₃	Bismuth acetate
Ba ₂ SO ₄	Barium sulfate
Bi ₂ O ₃	Bismuth oxide
BiBr ₃	Bismuth bromide
BiOBr	Bismuth oxide bromide
BzBr	Benzoyl bromide
CBM	Conduction band minima
CsBr	Cesium bromide
CS(OAc)	Cesium acetate
DFT	Density functional theory
DMF	Dimethylformamide
DMSO	Dimethyl sulfoxide
DOS	Density of state

DTG	Derivative thermogravimetry
EDX	Energy dispersive x-ray
ETL	Electron transport layer
EXAFS	Extended X-ray absorption fine structure
FESEM	Field-emission scanning electron microscopy
FTO	Fluorine-doped tin oxide
FWHM	Full-width half maximum
GBL	γ -butyrolactone
HBr	Hydrobromic acid
HIM	Hot-injection method
HTL	Hole transport layer
i-CRIM	Center for Research and Instrumentation Management
IPA	Isopropanol
IRF	Instrument respond factor
KBr	Potassium bromide
MABr	Methylammonium bromide
OA	Oleic acid
ODE	Octadecene
OLA	Oleylamine
PL	Photoluminescence spectroscopy
RM	Re-precipitation method
rpm	Rotation per minute
RR	Rietveld-refinement
TBABr	Tetrabutylammonium bromide
TDPL	Temperature-dependent photoluminescence spectroscopy
TGA	Thermogravimetric analysis
TiO ₂	Titanium dioxide

TMSBr	Trimethylsilyl bromide
TOPO	Trioctylphosphine
TRPL	Time-resolved photoluminescence spectroscopy
UPM	Universiti Putra Malaysia
UV-Vis	Ultraviolet-visible spectroscopy
VBM	Valence band maxima
WH	Williamson-Hall plot
XAFS	X-ray absorption fine structure spectroscopy
XANES	X-ray absorption near edge spectroscopy
XRD	X-ray diffraction

CHAPTER 1

INTRODUCTION

1.1 Overview of bismuth-based perovskite halides

Perovskite halides have emerged in recent years as a promising material for optoelectronic applications due to their low exciton binding energy, high carrier mobilities, versatility in material synthesis, and high diversification in materials structure (Dequilettes et al., 2019; Liu et al., 2020b; Ning et al., 2019; Zheng et al., 2015). Among these, lead-based perovskite has been extensively studied and performs well in solar cell and light-emitting diode applications, garnering significant attention from researchers (Miao et al., 2019; Turren-Cruz et al., 2018; Yang et al., 2016). However, the commercialization of lead-based perovskite is hampered by its toxicity and structural instability. Therefore, the discovery of lead-free materials exhibiting similar electronic properties to lead halide perovskites will be a critical step in the commercialization process.

Researchers are exploring the metal elements that are iso-valent to Pb^{2+} , such as germanium (Ge^{2+}) and tin (Sn^{2+}) to replace the lead-based perovskite materials. Germanium-based and tin-based perovskite materials exhibit a direct bandgap, excellent carrier mobility, and long diffusion length. In contrast, despite the favourable characteristics of Sn^{2+} and Ge^{2+} , they tend to undergo rapid degradation and oxidation into Sn^{4+} and Ge^{4+} under air conditions, respectively (Brandt et al., 2015). Furthermore, the search for alternatives to Pb^{2+} extends to hetero-valent metal cations

such as Tl^{3+} , Bi^{3+} , and Sb^{3+} . Nevertheless, it should be noted that Tl^+ have higher toxicity compared to lead and is prone to rapid degradation into Tl^{3+} upon exposure to air (Li et al., 2021a). While, both Sb^{3+} and Bi^{3+} are abundant and non-toxic compared to Pb^{2+} , and their single oxidation state makes them promising for achieving environmental stability (Jin et al., 2020; Li et al., 2021a; Sani et al., 2018).

Among all the bismuth-based perovskite materials, all inorganic Cs-Bi-Br based perovskite materials are reported to feature a superior structural stability as they composed solely of inorganic Cs^+ cation and Br^- anion that enhanced the thermodynamic of the materials structure, making them more robust and less prone to degradation while featuring a promising optical property (Luo et al., 2020; Xiao et al., 2016). Two different structures can be derived from the Cs-Bi-Br-based perovskite materials, that is the single perovskite ($\text{Cs}_3\text{Bi}_2\text{Br}_9$) and double perovskite ($\text{Cs}_2\text{AgBiBr}_6$) structure (Jin et al., 2020; Shi et al., 2020). Both of the perovskite structures feature exceptional and tunable optical properties that suit optoelectronic applications. Subsequently, the modification in the optical properties of Cs-Bi-Br-based perovskite materials is possible by employing compositional engineering and synthesis techniques.

The present study involved the optimization of a microwave-assisted solvothermal method to synthesize perovskite materials based on Cs-Bi-Br. The structural, morphological, optical, and thermal stability aspects of both pristine and MA^+ -substituted materials were investigated extensively. Additionally, the photovoltaic performance of all Cs-Bi-Br-based perovskite materials, including both pristine and MA^+ -substituted was evaluated. The findings of this study offer a novel pathway for

the synthesis of Cs-Bi-Br-based perovskite materials and provide a fundamental understanding of the effects of MA^+ -substitution on their properties for future photovoltaic applications.

1.2 Problem statement

The synthesis of perovskite materials based on Cs-Bi-Br is commonly achieved through the hot injection and re-precipitation method, which possesses both advantages and disadvantages. (Ahmad et al., 2021; Wu et al., 2021a; Zhou et al., 2018). The nucleation and crystal growth processes are separated in the hot injection method, enabling precise control over the material's particle size and morphology. Nevertheless, the hot injection method requires an inert atmosphere and a high-temperature reaction medium, complicating the experimental setup and limiting its applicability to organic-based studies (Ahmad et al., 2021; Wu et al., 2021a; Zhou et al., 2018). In contrast, the reprecipitation method benefits from its adaptable operating procedure and its room temperature process but is plagued by poor reproducibility. Therefore, it is essential to develop an alternative synthesis method with a simpler experimental setup, ensuring good reproducibility, and enabling organic-based studies of Cs-Bi-Br-based perovskite materials.

Generally, Cs-Bi-Br-based perovskite materials have been modified by engineering their composition through the A-site cation. The introduction of mixed A-site cation conditions in Cs-Bi-Br-based perovskite materials offers the potential to further adjust the energy bandgap and provide opportunities for carrier lifetime and strain engineering within the structure (Lee et al., 2022; Ünlü et al., 2020). However, current

research has predominantly focused on mixed inorganic A-site cations (Rb^+ , K^+ , Na^+ , Li^+) that are similar in size to Cs^+ in Cs-Bi-Br-based perovskite materials. Therefore, there is a pressing need to investigate mixed organic/inorganic A-site conditions for the future advancement of Cs-Bi-Br-based perovskite materials, as this strategy has the potential to improve optical properties while reserving material stability.

The following research questions have been addressed to justify the importance of the study:

1. What method is rapid, eco-friendly, features a simpler experimental setup, and enables organic-based studies of Cs-Bi-Br-based perovskite materials?
2. Why is the organic MA^+ cation chosen to improve the material characteristics in Cs-Bi-Br perovskite materials?
3. How does the substitution of MA^+ improve the photovoltaic performance of Bi-Br-based perovskite materials?

1.3 Hypotheses

The hypotheses based on the listed research questions are:

1. Microwave-assisted solvothermal method allows for rapid and environmentally friendly material synthesis (Gawande et al., 2014; Nayak et al., 2016). The method quickly converts electromagnetic waves into thermal energy, speeding up nucleation and particle growth without compromising quality. The experimental setup is simple, involving mixing reagents in a glass vial without needing an inert gas. Crucially, microwave-assisted solvothermal method is suitable for organic-based studies in Cs-Bi-Br-based perovskite

materials, as the reaction temperature conditions ($\leq 160^{\circ}\text{C}$) support mixed organic/inorganic perovskite formation. Therefore, microwave-assisted solvothermal method is ideal for synthesizing Cs-Bi-Br perovskite materials with mixed organic/inorganic A-site condition under optimized conditions.

2. The MA^+ organic cation, similar in size to Cs^+ , is favored over larger organic cations like ethylammonium and formamidinium for substituting the A-site cation in Cs-Bi-Br perovskite materials. Larger cations may cause phase segregation and increased lattice strain (Byranvand et al., 2022). The optimized substitution of MA^+ cation in Cs-Bi-Br-based perovskite materials is expected to integrate well into the Cs-Bi-Br perovskite structure, enhancing its structural stability and extending carrier lifespan. While excessive MA^+ cation substitution could lead to defects, the right amount is expected to reduce lattice strain, decrease the energy bandgap, prolong carrier lifetime, and enhance thermal stability.
3. The incorporation of MA^+ cation could cause a red-shifted bandgap and prolong the carrier lifetime of Cs-Bi-Br-based perovskite materials. Hence, it is expected that optimizing the MA^+ cation substitution could improve the photovoltaic performance of Cs-Bi-Br-based materials.

1.4 Objectives

Hence, based on the hypotheses mentioned above, the objectives of this study are:

1. to synthesize Cs-Bi-Br based single ($Cs_3Bi_2Br_9$) and double ($Cs_2AgBiBr_6$) perovskites via microwave-assisted solvothermal method.
2. to investigate the substitution effect of methylammonium (MA^+) organic cation on the structural, morphological, optical and thermal stability of Cs-Bi-Br-based perovskite.
3. to investigate the effect of MA^+ organic cation substitution on the photovoltaic application performance of Cs-Bi-Br-based perovskites.

1.5 Scope of study

This study optimized the synthesis process of Cs-Bi-Br-based perovskite materials, including single perovskite ($Cs_3Bi_2Br_9$) and double perovskite ($Cs_2AgBiBr_6$) via microwave-assisted solvothermal method. The synthesis parameters in the microwave-assisted solvothermal method such as solvents (isopropanol, hexane), ligands (oleylamine, oleic acid) and additive (hydrobromic acid) are optimized based on the materials. The material's structural, morphological, optical and thermal stability of pristine $Cs_3Bi_2Br_9$ and $Cs_2AgBiBr_6$ materials were investigated. Furthermore, the $Cs_3Bi_2Br_9$ and $Cs_2AgBiBr_6$ materials were subject to MA^+ substitution, aiming to investigate the impact of MA^+ substitution on the structural, morphological, optical, and thermal stability of perovskite materials. Finally, the synthesized perovskite materials were subjected to the photovoltaic application, regardless of pristine or MA^+ substituted $Cs_3Bi_2Br_9$ and $Cs_2AgBiBr_6$ materials.

1.6 Thesis outline

This thesis is composed of 5 chapters. A general introduction to Cs-Bi-Br perovskite materials and the objectives of the study were presented in chapter one. Recent progress in the bismuth-based perovskite materials, including properties and synthesis methods of Cs-Bi-Br-based perovskite were outlined in chapter two. All the experimental synthesis and materials characterizations of Cs-Bi-Br-based perovskite materials were described in chapter three. Following that, all the results acquired for Cs-Bi-Br-based perovskite materials to achieve the study objectives were presented and discussed in chapter four. Finally, all the research findings and future perspectives of the study were concluded in chapter five.

REFERENCES

- Aamir, M., Sher, M., & Akhtar, J. (2023). Synthesis of lead free hybrid copper halide perovskite nanosheets: Structural and optical properties. *Results in Optics*, 13, 100562.
- Absike, H., Baaalla, N., Lamouri, R., Labrim, H., & Ez-zahraouy, H. (2022). Optoelectronic and photovoltaic properties of $\text{Cs}_2\text{AgBiX}_6$ ($X = \text{Br}$, Cl , or I) halide double perovskite for solar cells: insight from density functional theory. *International Journal of Energy Research*, 46(8), 11053-11064.
- Adamo, C., & Barone, V. (1999). Toward reliable density functional methods without adjustable parameters: the PBE0 model. *The Journal of Chemical Physics*, 110(13), 6158-6170.
- Ahmad, R., Nutan, G. V., Singh, D., Gupta, G., Soni, U., Sapra, S., & Srivastava, R. (2021). Colloidal lead-free $\text{Cs}_2\text{AgBiBr}_6$ double perovskite nanocrystals: Synthesis, uniform thin-film fabrication, and application in solution-processed solar cells. *Nano Research*, 14, 1126-1134.
- Ahn, C. W., Jo, J. H., Choi, J. S., Hwang, Y. H., Kim, I. W., & Kim, T. H. (2023). Heteroanionic lead-free double-perovskite halides for bandgap engineering. *Advanced Engineering Materials*, 25(1), 2201119.
- Akinbami, O., Moepya, R., Ngubeni, G. N., Tetyana, P., Mubiayi, K. P., Moloto, M. J., & Moloto, N. (2021). Lead-free rudorffite-type $\text{Cs}_3\text{Bi}_2\text{Br}_9$ nanoparticles for photocatalytic degradation of rhodamine B and methylene blue. *Journal of Photochemistry and Photobiology A: Chemistry*, 419, 113460.
- Albarri, R., Toprakçı, İ., Kurtulbaş, E., & Şahin, S. (2023). Estimation of diffusion and mass transfer coefficients for the microwave-assisted extraction of bioactive substances from *Moringa oleifera* leaves. *Biomass Conversion and Biorefinery*, 13, 5125-5132.
- Aleksandrova, I. P., Burriel, R., Bartolome, J., Bagautdinov, B. S., Blasco, J., Sukhovsky, A. A., Torres, J. M., Vasiljev, A. D., & Solovjev, L. A. (2002). Low-temperature phase transitions in the trigonal modification of $\text{Cs}_3\text{Bi}_2\text{Br}_9$ and $\text{Cs}_3\text{Sb}_2\text{I}_9$. *Phase Transitions*, 75(6), 607-620.
- Ali, R. F., Andreu, I., & Gates, B. D. (2019). Green solvent assisted synthesis of cesium bismuth halide perovskite nanocrystals and the influences of slow and fast anion exchange rates. *Nanoscale Advances*, 1(11), 4442-4449.
- Alshogeathri, S., Cao, D., Kim, D., & Yang, G. (2023). Gel growth and characterization of $\text{Cs}_3\text{Bi}_2\text{Br}_9$ perovskite single crystals for radiation detection. *Frontiers in Physics*, 11, 1129301.
- Amat, A., Mosconi, E., Ronca, E., Quarti, C., Umari, P., Nazeeruddin, M. K., Grätzel, M., & De Angelis, F. (2014). Cation-induced band-gap tuning in organohalide perovskites: interplay of spin-orbit coupling and octahedra tilting. *Nano Letters*, 14(6), 3608-3616.

- An, Y., Hidalgo, J., Perini, C. A. R., Castro-Méndez, A. F., Vagott, J. N., Bairley, K., Wang, S., Li, X., & Correa-Baena, J. P. (2021). Structural stability of formamidinium and cesium-based halide perovskites. *ACS Energy Letters*, 6(5), 1942-1969.
- Arain, Z., Liu, C., Yang, Y., Mateen, M., Ren, Y., Ding, Y., Liu, X., Ali, Z., Kumar, M., & Dai, S. (2019). Elucidating the dynamics of solvent engineering for perovskite solar cells. *Science China Materials*, 62(2), 161-172.
- Bai, Z. J., Mao, Y., Wang, B. H., Chen, L., Tian, S., Hu, B., Li, Y. J., Au, C. T., & Yin, S. F. (2022). Tuning photocatalytic performance of $\text{Cs}_3\text{Bi}_2\text{Br}_9$ perovskite by $\text{g-C}_3\text{N}_4$ for $\text{C}(\text{sp}^3)$ —H bond activation. *Nano Research*, 16(5), 6104-6112.
- Bass, K. K., Estergreen, L., Savory, C. N., Buckeridge, J., Scanlon, D. O., Djurovich, P. I., Bradforth, S. E., Thompson, M. E., & Melot, B. C. (2017). Vibronic structure in room temperature photoluminescence of the halide perovskite $\text{Cs}_3\text{Bi}_2\text{Br}_9$. *Inorganic Chemistry*, 56(1), 42-45.
- Bearden, J. A., & Burr, A. F. (1967). Reevaluation of X-ray atomic energy levels. *Reviews of Modern Physics*, 39(1), 125.
- Bekenstein, Y., Dahl, J. C., Huang, J., Osowiecki, W. T., Swabeck, J. K., Chan, E. M., Yang, P., & Alivisatos, A. P. (2018). The making and breaking of lead-free double perovskite nanocrystals of cesium silver-bismuth halide compositions. *Nano Letters*, 18(6), 3502-3508.
- Bellakhdar, T., Nabi, Z., Bouabdallah, B., Benichou, B., & Saci, H. (2022). Ab initio study of structural, electronic, mechanical and optical properties of the tetragonal $\text{Cs}_2\text{AgBiBr}_6$ halide double perovskite. *Applied Physics A: Materials Science and Processing*, 128(2), 155.
- Bhattacharjee, S., Chaudhary, S. P., & Bhattacharyya, S. (2019). Lead-free metal halide perovskite nanocrystals for photocatalysis in water. *ChemRxiv*, 1, 1-27.
- Bi, C., Wang, S., Li, Q., Kershaw, S. V., Tian, J., & Rogach, A. L. (2019). Thermally stable copper (II)-doped cesium lead halide perovskite quantum dots with strong blue emission. *Journal of Physical Chemistry Letters*, 10(5), 943-952.
- Biswas, A., & Islam, M. R. (2021). Optical properties of mixed-halide double perovskites $\text{Cs}_2\text{AgBi}(\text{Br}_{1-x}\text{I}_x)_6$: first-principle study. In 2021 5th International Conference on Electrical Information and Communication Technology (EICT), 1-6.
- Botton, G., & Prabhudev, S. (2019). Analytical electron microscopy. In P. W. Hawkes & J. C. H. Spence (Eds.), *Springer handbook of microscopy* (pp. 345-453). Springer International Publishing.
- Brandt, R. E., Stevanović, V., Ginley, D. S., & Buonassisi, T. (2015). Identifying defect-tolerant semiconductors with high minority-carrier lifetimes: beyond hybrid lead halide perovskites. *MRS Communications*, 5(2), 265-275.

- Burwig, T., Guc, M., Izquierdo-Roca, V., & Pistor, P. (2020). Synthesis and crystal structure evolution of co-evaporated $\text{Cs}_2\text{AgBiBr}_6$ thin films upon thermal treatment. *Journal of Physical Chemistry C*, 124(17), 9249-9255.
- Byranvand, M. M., Otero-Martínez, C., Ye, J., Zuo, W., Manna, L., Saliba, M., Hoye, R. L. Z., & Polavarapu, L. (2022). Recent progress in mixed A-site cation halide perovskite thin-films and nanocrystals for solar cells and light-emitting diodes. *Advanced Optical Materials*, 10(14), 2200423.
- Dakshinamurthy, A. C., & Sudakar, C. (2022). Photoinduced degradation of thermally stable $\text{Cs}_2\text{AgBiBr}_6$ double perovskites by micro-Raman studies. *Materials Advances*, 3(14), 5813-5817.
- Cai, T., Shi, W., Hwang, S., Kobbekaduwa, K., Nagaoka, Y., Yang, H., Hills-Kimball, K., Zhu, H., Wang, J., Wang, Z., Liu, Y., Su, D., Gao, J., & Chen, O. (2020). Lead-free $\text{Cs}_4\text{CuSb}_2\text{Cl}_{12}$ layered double perovskite nanocrystals. *Journal of the American Chemical Society*, 142(27), 11927-11936.
- Cao, Y., Zhang, Z., Li, L., Zhang, J. R., & Zhu, J. J. (2019). An improved strategy for high-quality cesium bismuth bromine perovskite quantum dots with remarkable electrochemiluminescence activities. *Analytical Chemistry*, 91(13), 8607-8614.
- Ceperley, D. M., & Alder, B. J. (1980). Ground state of the electron gas by a stochastic method. *Physical Review Letters*, 45(7), 566.
- Chao, L., Niu, T., Gao, W., Ran, C., Song, L., Chen, Y., & Huang, W. (2021). Solvent engineering of the precursor solution toward large-area production of perovskite solar cells. *Advanced Materials*, 33(14), 2005410.
- Che Hak, C. R., Choo, T. F., Othman, N. A. F., Shukri, N. A., Ripin, M. S., Meor Sulaiman, M. Y., & Abdullah, Y. (2015). Field Emission Scanning Electron Microscope (FESEM) Facility in BTI. Paper presented at the Nuclear Technical Convention 2015, Malaysia.
- Chen, B., Rudd, P. N., Yang, S., Yuan, Y., & Huang, J. (2019a). Imperfections and their passivation in halide perovskite solar cells. *Chemical Society Reviews*, 48(14), 3842-3867.
- Chen, H., Zhang, C. R., Liu, Z. J., Gong, J. J., Zhang, M. L., Wu, Y. Z., Chen, Y. H., & Chen, H. S. (2021). Optoelectronic properties of Rb-doped inorganic double perovskite $\text{Cs}_2\text{AgBiBr}_6$. *Chemical Physics Letters*, 771, 138501.
- Chen, J., Wu, M., Ni, J., & Ni, C. (2023). Br vacancy engineering in $\text{Cs}_3\text{Bi}_2\text{Br}_9$ for photocatalytic NO oxidation under visible light. *Environmental Science and Pollution Research*, 30(19), 56188–56197.
- Chen, N., Cai, T., Li, W., Hills-Kimball, K., Yang, H., Que, M., Nagaoka, Y., Liu, Z., Yang, D., Dong, A., Xu, C. Y., Zia, R., & Chen, O. (2019b). Yb- and Mn-doped lead-free double perovskite $\text{Cs}_2\text{AgBiX}_6$ ($X = \text{Cl}^-$, Br^-) nanocrystals. *ACS Applied Materials and Interfaces*, 11(18), 16855-16863.

- Chen, T., Chen, W. L., Foley, B. J., Lee, J., Ruff, J. P. C., Ko, J. Y. P., Brown, C. M., Harriger, L. W., Zhang, D., Park, C., Yoon, M., Chang, Y. M., Choi, J. J., & Lee, S. H. (2017). Origin of long lifetime of band-edge charge carriers in organic-inorganic lead iodide perovskites. *Proceedings of the National Academy of Sciences of the United States of America*, 114(29), 7519-7524.
- Chen, Y. L., Yan, D. N., Zeng, M. W., Liao, C. S., & Cai, M. Q. (2022). 2D and 3D double perovskite with dimensionality-dependent optoelectronic properties: First-principle study on $\text{Cs}_2\text{AgBiBr}_6$ and $\text{Cs}_4\text{AgBiBr}_8$. *Journal of Physics Condensed Matter*, 34(6), 065510.
- Chini, M. K., Goverapet Srinivasan, S., Tailor, N. K., Yukta, Salahub, D., & Satapathi, S. (2020). Lead-free, stable mixed halide double perovskites $\text{Cs}_2\text{AgBiBr}_6$ and $\text{Cs}_2\text{AgBiBr}_{6-x}\text{Cl}_x$ – a detailed theoretical and experimental study. *Chemical Physics*, 529, 110547.
- Cohen, A., Brenner, T. M., Klarbring, J., Sharma, R., Fabini, D. H., Korobko, R., Nayak, P. K., Hellman, O., & Yaffe, O. (2022). Diverging expressions of anharmonicity in halide perovskites. *Advanced Materials*, 34(14), 2107932.
- Connor, B. A., Leppert, L., Smith, M. D., Neaton, J. B., & Karunadasa, H. I. (2018). Layered halide double perovskites: dimensional reduction of $\text{Cs}_2\text{AgBiBr}_6$. *Journal of the American Chemical Society*, 140(15), 5235-5240.
- Creutz, S. E., Crites, E. N., De Siena, M. C., & Gamelin, D. R. (2018). Colloidal nanocrystals of lead-free double-perovskite (elpasolite) semiconductors: synthesis and anion exchange to access new materials. *Nano Letters*, 18(2), 1118-1123.
- Creutz, S. E., Liu, H., Kaiser, M. E., Li, X., & Gamelin, D. R. (2019). Structural diversity in cesium bismuth halide nanocrystals. *Chemistry of Materials*, 31(13), 4685-4697.
- da Silva, T. C., Fernández-Saiz, C., Sánchez, R. S., Gualdrón-Reyes, A. F., Mora-Seró, I., & Julián-López, B. (2023). A soft-chemistry route to prepare halide perovskite nanocrystals with tunable emission and high optical performance. *Journal of Sol-Gel Science and Technology*, 1-8.
- Dai, Y., & Tüysüz, H. (2019). Lead-free $\text{Cs}_3\text{Bi}_2\text{Br}_9$ perovskite as photocatalyst for ring-opening reactions of epoxides. *ChemSusChem*, 12(12), 2587-2592.
- Dai, Y., & Tüysüz, H. (2021). Rapid acidic media growth of $\text{Cs}_3\text{Bi}_2\text{Br}_9$ halide perovskite platelets for photocatalytic toluene oxidation. *Solar RRL*, 5(7), 2100265.
- De Roo, J., Ibáñez, M., Geiregat, P., Nedelcu, G., Walravens, W., Maes, J., Martins, J. C., Van Driessche, I., Kovalenko, M. V., & Hens, Z. (2016). Highly dynamic ligand binding and light absorption coefficient of cesium lead bromide perovskite nanocrystals. *ACS Nano*, 10(2), 2071-2081.
- Dequilettes, D. W., Frohma, K., Emin, D., Kirchartz, T., Bulovic, V., Ginger, D. S., & Stranks, S. D. (2019). Charge-carrier recombination in halide perovskites: focus review. *Chemical Reviews*, 119(20), 11007-11019.

- Dey, A., Richter, A. F., Debnath, T., Huang, H., Polavarapu, L., & Feldmann, J. (2020). Transfer of direct to indirect bound excitons by electron intervalley scattering in $\text{Cs}_2\text{AgBiBr}_6$ double perovskite nanocrystals. *ACS Nano*, 4(5), 5855-5861.
- Ding, N., Zhou, D., Pan, G., Xu, W., Chen, X., Li, D., Zhang, X., Zhu, J., Ji, Y., & Song, H. (2019). Europium-doped lead-free $\text{Cs}_3\text{Bi}_2\text{Br}_9$ perovskite quantum dots and ultrasensitive Cu^{2+} detection. *ACS Sustainable Chemistry and Engineering*, 7(9), 8397-8404.
- Djokić, V., Andričević, P., Kollár, M., Ciers, A., Arakcheeva, A., Vasiljević, M., Damjanović, D., Forró, L., Horváth, E., & Ivšić, T. (2022). Fast lead-free humidity sensor based on hybrid halide perovskite. *Crystals*, 12(4), 547.
- Dror, S., Khalfin, S., Veber, N., Lang, A., Kauffmann, Y., Koifman Khristosov, M., Shechter, R., Pokroy, B., Castelli, I. E., & Bekenstein, Y. (2023). Transformations of 2D to 3D double-perovskite nanoplates of $\text{Cs}_2\text{AgBiBr}_6$ composition. *Chemistry of Materials*, 35(3), 1363-1372.
- Du, K. Z., Meng, W., Wang, X., Yan, Y., & Mitzi, D. B. (2017). Bandgap engineering of lead-free double perovskite $\text{Cs}_2\text{AgBiBr}_6$ through trivalent metal alloying. *Angewandte Chemie International Edition*, 56(28), 8158-8162.
- Duan, M., Wang, Y., Zhang, P., & Du, L. (2023). Effect of Cs^+ doping on the carrier dynamics of MAPbI_3 perovskite. *Materials*, 16(17), 6064.
- Elattar, A., Kobera, L., Kangsabanik, J., Suzuki, H., Abbrent, S., Nishikawa, T., Thygesen, K. S., Brus, J., & Hayashi, Y. (2022). Structure modulation for bandgap engineered vacancy-ordered $\text{Cs}_3\text{Bi}_2\text{Br}_9$ perovskite structures through copper alloying. *Journal of Materials Chemistry C*, 10(35), 12863-12872.
- Fang, H. H., Wang, F., Adjokatse, S., Zhao, N., Even, J., & Loi, M. A. (2016). Photoexcitation dynamics in solution-processed formamidinium lead iodide perovskite thin films for solar cell applications. *Light: Science and Applications*, 5(4), e16056–e16056.
- Feria, D. N., Su, J. W., Wu, G. H., Zeng, Y. T., Lian, J. T., & Lin, T. Y. (2023). Revealing the enhanced crystalline quality mechanism of perovskites produced by microwave-assisted synthesis: toward the fabrications in a fully ambient air environment. *Materials Today Sustainability*, 24, 100532.
- Fernández-Castillejo, S., Pedret Figuerola, A., Catalán Santos, Ú., Motta, C., & Solà, R. (2022). Monitoring the anisotropy and fluidity of the HDL monolayer as surrogates of HDL functionality. In D. Ramji (Ed.), *Atherosclerosis. Methods in Molecular Biology*, vol 2419 (pp. 275-282). Humana, New York, NY.
- Filip, M. R., Hillman, S., Haghaghirad, A. A., Snaith, H. J., & Giustino, F. (2016). Band gaps of the lead-free halide double perovskites $\text{Cs}_2\text{BiAgCl}_6$ and $\text{Cs}_2\text{BiAgBr}_6$ from theory and experiment. *Journal of Physical Chemistry Letters*, 7(13), 2579-2585.

- Frebel, A., Yoon, S., Meles Neguse, S., Jöckel, D. M., Widenmeyer, M., Lange, S., Naumann, V., Rosspeintner, A., Ebbinghaus, S. G., Balke, B., & Weidenkaff, A. (2022). Controlling the defects of $\text{Cs}_2\text{AgBiBr}_6$ by varied precursor compositions. *Advanced Photonics Research*, 3(11), 2200061.
- Fu, R., Chen, Y., Yong, X., Ma, Z., Wang, L., Lv, P., Lu, S., Xiao, G., & Zou, B. (2019). Pressure-induced structural transition and band gap evolution of double perovskite $\text{Cs}_2\text{AgBiBr}_6$ nanocrystals. *Nanoscale*, 11(36), 17004–17009.
- Gao, M., Zhang, C., Lian, L., Guo, J., Xia, Y., Pan, F., Su, X., Zhang, J., Li, H., & Zhang, D. (2019). Controlled synthesis and photostability of blue emitting $\text{Cs}_3\text{Bi}_2\text{Br}_9$ perovskite nanocrystals by employing weak polar solvents at room temperature. *Journal of Materials Chemistry C*, 7(12), 3688–3695.
- García-Espejo, G., Rodríguez-Padrón, D., Luque, R., Camacho, L., & De Miguel, G. (2019). Mechanochemical synthesis of three double perovskites: $\text{Cs}_2\text{AgBiBr}_6$, $(\text{CH}_3\text{NH}_3)_2\text{TlBiBr}_6$ and $\text{Cs}_2\text{AgSbBr}_6$. *Nanoscale*, 11(35), 16650–16657.
- Gawande, M. B., Shelke, S. N., Zboril, R., & Varma, R. S. (2014). Microwave-assisted chemistry: synthetic applications for rapid assembly of nanomaterials and organics. *Accounts of Chemical Research*, 47(4), 1338–1348.
- Geng, H., Huang, Z., Geng, H., Liu, S., Naumova, M. A., Salvia, R., Chen, S., Wei, J., Zhang, L., Zou, X., Lin, W., Cai, X., Yuan, M., Hu, Z., Shen, X., Yu, R., Zheng, K., Canton, S. E., & Fu, X. (2023). Controlled synthesis of highly stable lead-free bismuth halide perovskite nanocrystals: Structures and photophysics. *Science China Materials*, 66, 2079–2089.
- Geng, T., Wei, S., Zhao, W., Ma, Z., Fu, R., Xiao, G., & Zou, B. (2021). Insight into the structure-property relationship of two-dimensional lead-free halide perovskite $\text{Cs}_3\text{Bi}_2\text{Br}_9$ nanocrystals under pressure. *Inorganic Chemistry Frontiers*, 8(6), 1410–1415.
- Ghimire, S., Rehhagen, C., Fiedler, S., Parekh, U., Lesyuk, R., Lochbrunner, S., & Klinke, C. (2022). Synthesis, optoelectronic properties, and charge carrier dynamics of colloidal quasi-twodimensional $\text{Cs}_3\text{Bi}_2\text{I}_9$ perovskite nanosheets. *Nanoscale*, 15(5), 2096–2105.
- Ghosh, S., Mukhopadhyay, S., Paul, S., Pradhan, B., & De, S. K. (2020). Control synthesis and alloying of ambient stable Pb-free $\text{Cs}_3\text{Bi}_2\text{Br}_{9(1-x)}\text{I}_{9x}$ ($0 \leq x \leq 1$) perovskite nanocrystals for photodetector application. *ACS Applied Nano Materials*, 3(11), 11107–11117.
- Ghosh, S., Rana, D., Pradhan, B., Donfack, P., Hofkens, J., & Materny, A. (2021). Vibrational study of lead bromide perovskite materials with variable cations based on Raman spectroscopy and density functional theory. *Journal of Raman Spectroscopy*, 52(12), 2338–2347.

- Giovilli, G., Albini, B., Grisci, V., Bonomi, S., Moroni, M., Mosconi, E., Kaiser, W., De Angelis, F., Galinetto, P., & Malavasi, L. (2023). Band gap tuning through cation and halide alloying in mechanochemical synthesized $\text{Cs}_3(\text{Sb}_{1-x}\text{Bi}_x)_2\text{Br}_9$ and $\text{Cs}_3\text{Sb}_2(\text{I}_{1-x}\text{Br}_x)_9$ solid solutions. *Journal of Materials Chemistry C*, 11(30), 10282-10291.
- Girdzis, S. P., Lin, Y., Leppert, L., Slavney, A. H., Park, S., Chapman, K. W., Karunadasa, H. I., & Mao, W. L. (2021). Revealing local disorder in a silver-bismuth halide perovskite upon compression. *Journal of Physical Chemistry Letters*, 12(1), 532-536.
- Goldstein, J. I., Newbury, D. E., Michael, J. R., Ritchie, N. W. M., Scott, J. H. J., & Joy, D. C. (2017). *Scanning Electron Microscopy and X-Ray Microanalysis* (4th ed., pp. 1-172). New York, NY: Springer New York.
- Gray, M. B., McClure, E. T., & Woodward, P. M. (2019). $\text{Cs}_2\text{AgBiBr}_{6-x}\text{Cl}_x$ solid solutions -band gap engineering with halide double perovskites. *Journal of Materials Chemistry C*, 7(31), 9686-9689.
- Grewal, A. S., Kumar, K., Redhu, S., & Bhardwaj, S. (2013). Microwave assisted synthesis: a green chemistry approach. *International Research Journal of Pharmaceutical and Applied Sciences*, 3(5), 278-285.
- Guechi, N., Bouhemadou, A., Bin-Omran, S., Bourzami, A., & Louail, L. (2018). Elastic, optoelectronic and thermoelectric properties of the lead-free halide semiconductors $\text{Cs}_2\text{AgBiX}_6$ ($X = \text{Cl}, \text{Br}$): ab initio investigation. *Journal of Electronic Materials*, 47(2), 1533-1545.
- Gull, S., Jamil, M. H., Zhang, X., Kwok, H. sing, & Li, G. (2022). Stokes shift in inorganic lead halide perovskites: current status and perspective. *ChemistryOpen*, 11(3), e202100285.
- Hadi, M. A., Islam, M. N., & Podder, J. (2022). Indirect to direct band gap transition through order to disorder transformation of $\text{Cs}_2\text{AgBiBr}_6$ via creating antisite defects for optoelectronic and photovoltaic applications. *RSC Advances*, 12(24), 15461-15469.
- Hamill, J. C., Schwartz, J., & Loo, Y. L. (2018). Influence of solvent coordination on hybrid organic-inorganic perovskite formation. *ACS Energy Letters*, 3(1), 92-97.
- Han, D., Zhang, T., Huang, M., Sun, D., Du, M. H., & Chen, S. (2018). Predicting the thermodynamic stability of double-perovskite halides from density functional theory. *APL Materials*, 6(8), 084902.
- Han, P., Mao, X., Yang, S., Zhang, F., Yang, B., Wei, D., Deng, W., & Han, K. (2019a). Lead-free sodium-indium double perovskite nanocrystals through doping silver cations for bright yellow emission. *Angewandte Chemie*, 131(48), 17391-17395.
- Han, P., Zhang, X., Luo, C., Zhou, W., Yang, S., Zhao, J., Deng, W., & Han, K. (2020). Manganese-doped, lead-free double perovskite nanocrystals for bright orange-red emission. *ACS Central Science*, 6(4), 566-572.

- Han, P., Zhang, X., Mao, X., Yang, B., Yang, S., Feng, Z., Wei, D., Deng, W., Pullerits, T., & Han, K. (2019b). Size effect of lead-free halide double perovskite on luminescence property. *Science China Chemistry*, 62, 1405-1413.
- Hao, M., Zhang, J., Zhang, X. H., & Chua, S. (2002). Photoluminescence studies on InGaN/GaN multiple quantum wells with different degree of localization. *Applied Physics Letters*, 81(27), 5129-5131.
- Hardcastle, F. D., & Wachs, I. E. (1992). The molecular structure of bismuth oxide by Raman spectroscopy. *Journal of Solid State Chemistry*, 97(2), 319-331.
- Harrison, S. (2016). Exploring and exploiting charge-carrier confinement in semiconductor nanostructures: heterodimensionality in sub-monolayer InAs in GaAs and photoelectrolysis using type-II heterojunctions [Doctoral dissertation, Lancaster University]. Lancaster University Library.
- Hazarika, A., Zhao, Q., Ashley Gaulding, E., Christians, J. A., Dou, B., Marshall, A. R., Moot, T., Berry, J. J., Johnson, J. C., & Luther, J. M. (2018). Perovskite quantum dot photovoltaic materials beyond the reach of thin films: full-range tuning of A-site cation composition. *ACS Nano*, 12(10), 10327-10337.
- He, H., Yu, Q., Li, H., Li, J., Si, J., Jin, Y., Wang, N., Wang, J., He, J., Wang, X., Zhang, Y. & Ye, Z. (2016). Exciton localization in solution-processed organolead trihalide perovskites. *Nature communications*, 7(1), 10896.
- Hewat, A., David, W. I. F., & van Eijck, L. (2016). Hugo Rietveld (1932–2016). *Journal of Applied Crystallography*, 49(4), 1394–1395.
- Heyd, J., Scuseria, G. E., & Ernzerhof, M. (2006). Hybrid functionals based on a screened coulomb potential. *The Journal of Chemical Physics*, 124, 219906.
- Hodgkins, T. L., Savory, C. N., Bass, K. K., Seckman, B. L., Scanlon, D. O., Djurovich, P. I., Thompson, M. E., & Melot, B. C. (2019). Anionic order and band gap engineering in vacancy ordered triple perovskites. *Chemical Communications*, 55(21), 3164-3167.
- Hong, K. H., Kim, J., Debbichi, L., Kim, H., & Im, S. H. (2017). Band gap engineering of Cs₃Bi₂I₉ perovskites with trivalent atoms using a dual metal cation. *Journal of Physical Chemistry C*, 121(1), 969-974.
- Hou, P., Yang, W., Wan, N., Fang, Z., Zheng, J., Shang, M., Fu, D., Yang, Z., & Yang, W. (2021). Precursor engineering for high-quality Cs₂AgBiBr₆ films toward efficient lead-free double perovskite solar cells. *Journal of Materials Chemistry C*, 9(30), 9659-9669.
- Hoyle, R. L. Z., Eyre, L., Wei, F., Brivio, F., Sadhanala, A., Sun, S., Li, W., Zhang, K. H. L., MacManus-Driscoll, J. L., Bristowe, P. D., Friend, R. H., Cheetham, A. K., & Deschler, F. (2018). Fundamental carrier lifetime exceeding 1 μs in Cs₂AgBiBr₆ double perovskite. *Advanced Materials Interfaces*, 5(15), 1800464.

- Hu, Q., Niu, G., Zheng, Z., Li, S., Zhang, Y., Song, H., Zhai, T., & Tang, J. (2019). Tunable color temperatures and efficient white emission from $\text{Cs}_2\text{Ag}_{1-x}\text{Na}_x\text{In}_{1-y}\text{Bi}_y\text{Cl}_6$ double perovskite nanocrystals. *Small*, 15(44), 1903496.
- Huang, J., Zou, S., Lin, J., Liu, Z., & Qi, M. (2021). Ultrathin lead-free double perovskite cesium silver bismuth bromide nanosheets. *Nano Research*, 14(11), 4079-4086.
- Hutter, E. M., Gélvez-Rueda, M. C., Bartesaghi, D., Grozema, F. C., & Savenije, T. J. (2018). Band-like charge transport in $\text{Cs}_2\text{AgBiBr}_6$ and mixed antimony-bismuth $\text{Cs}_2\text{AgBi}_{1-x}\text{Sb}_x\text{Br}_6$ halide double perovskites. *ACS Omega*, 3(9), 11655-11662.
- Igbari, F., Wang, R., Wang, Z. K., Ma, X. J., Wang, Q., Wang, K. L., Zhang, Y., Liao, L. S., & Yang, Y. (2019). Composition stoichiometry of $\text{Cs}_2\text{AgBiBr}_6$ films for highly efficient lead-free perovskite solar cells. *Nano Letters*, 19(3), 2066-2073.
- Imani, R., Borca, C. H., Pazoki, M., & Edvinsson, T. (2022). Excited-state charge polarization and electronic structure of mixed-cation halide perovskites: the role of mixed inorganic-organic cations in CsFAPbI_3 . *RSC Advances*, 12(39), 25415-25423.
- Islam, M. N., Podder, J., Saha, T., & Rani, P. (2021). Semiconductor to metallic transition under induced pressure in $\text{Cs}_2\text{AgBiBr}_6$ double halide perovskite: a theoretical DFT study for photovoltaic and optoelectronic applications. *RSC Advances*, 11(39), 24001-24012.
- Ito, B. I., Tekelenburg, E. K., Blake, G. R., Loi, M. A., & Nogueira, A. F. (2021). Double perovskite single-crystal photoluminescence quenching and resurgence: the role of Cu doping on its photophysics and crystal structure. *Journal of Physical Chemistry Letters*, 12(42), 10444-10449.
- Ivanov, Y. N., Sukhovskii, A. A., Lisin, V. V., & Aleksandrova, I. P. (2001). Phase transitions of $\text{Cs}_3\text{Sb}_2\text{I}_9$, $\text{Cs}_3\text{Bi}_2\text{I}_9$, and $\text{Cs}_3\text{Bi}_2\text{Br}_9$ crystals. *Inorganic Materials*, 37, 623-627.
- Jancik, J., Jancik Prochazkova, A., Scharber, M. C., Kovalenko, A., Máslík, J., Sarıçiftci, N. S., Weiter, M. & Krajcovic, J. (2020). Microwave-assisted preparation of organo-lead halide perovskite single crystals. *Crystal growth & design*, 20(3), 1388-1393.
- Ji, F., Huang, Y., Wang, F., Kobera, L., Xie, F., Klarbring, J., Abbrent, S., Brus, J., Yin, C., Simak, S. I., Abrikosov, I. A., Buyanova, I. A., Chen, W. M., & Gao, F. (2020a). Near-infrared light-responsive Cu-doped $\text{Cs}_2\text{AgBiBr}_6$. *Advanced Functional Materials*, 30(51), 2005521.
- Ji, F., Klarbring, J., Wang, F., Ning, W., Wang, L., Yin, C., Figueroa, J. S. M., Christensen, C. K., Etter, M., Ederth, T., Sun, L., Simak, S. I., Abrikosov, I. A., & Gao, F. (2020b). Lead-free halide double perovskite $\text{Cs}_2\text{AgBiBr}_6$ with decreased band gap. *Angewandte Chemie*, 132(35), 15303-15306.

- Ji, F., Wang, F., Kobera, L., Abbrent, S., Brus, J., Ning, W., & Gao, F. (2021). The atomic-level structure of bandgap engineered double perovskite alloys $\text{Cs}_2\text{AgIn}_{1-x}\text{Fe}_x\text{Cl}_6$. *Chemical Science*, 12(5), 1730-1735.
- Ji, Y., She, M., Bai, X., Liu, E., Xue, W., Zhang, Z., Wan, K., Liu, P., Zhang, S., & Li, J. (2022). In-depth understanding of the effect of halogen-induced stable 2D bismuth-based perovskites for photocatalytic hydrogen evolution activity. *Advanced Functional Materials*, 32(31), 2201721.
- Ji, Z., Liu, Y., Li, W., Zhao, C., & Mai, W. (2020c). Reducing current fluctuation of $\text{Cs}_3\text{Bi}_2\text{Br}_9$ perovskite photodetectors for diffuse reflection imaging with wide dynamic range. *Science Bulletin*, 65(16), 1371-1379.
- Jia, X., Liu, Y., Bhatt, P., Perry, R. S., Parkin, I. P., & Palgrave, R. G. (2023). Mixed valence Sn doped $(\text{CH}_3\text{NH}_3)_3\text{Bi}_2\text{Br}_9$ produced by mechanochemical synthesis. *Physical Chemistry Chemical Physics*, 25(6), 4563-4569.
- Jiang, Z., Liu, H., Zou, J., Huang, Y., Xu, Z., Pustovyi, D., & Vitusevich, S. (2023). Scale-up synthesis of high-quality solid-state-processed CsCuX ($X = \text{Cl}, \text{Br}, \text{I}$) perovskite nanocrystal materials toward near-ultraviolet flexible electronic properties. *RSC Advances*, 13(9), 5993-6001.
- Jin, Z., Zhang, Z., Xiu, J., Song, H., Gatti, T., & He, Z. (2020). A critical review on bismuth and antimony halide based perovskites and their derivatives for photovoltaic applications: recent advances and challenges. *Journal of Materials Chemistry A*, 8(32), 16166-16188.
- Ju, D., Jiang, X., Xiao, H., Chen, X., Hu, X., & Tao, X. (2018). Narrow band gap and high mobility of lead-free perovskite single crystal Sn-doped $\text{MA}_3\text{Sb}_2\text{I}_9$. *Journal of Materials Chemistry A*, 6(42), 20753-20759.
- Juarez-Perez, E. J., Ono, L. K., & Qi, Y. (2019). Thermal degradation of formamidinium based lead halide perovskites into sym-triazine and hydrogen cyanide observed by coupled thermogravimetry-mass spectrometry analysis. *Journal of Materials Chemistry A*, 7(28), 16912-16919.
- Kandel, R., Schatte, G., Cheng, G., Palmer, C., Beauchemin, D., & Wang, P. L. (2020). Stabilization and solvent driven crystal-to-crystal transition between new bismuth halides. *Inorganic Chemistry*, 59(10), 7049-7055.
- Kentsch, R., Scholz, M., Horn, J., Schlettwein, D., Oum, K., & Lenzer, T. (2018). Exciton dynamics and electron-phonon coupling affect the photovoltaic performance of the $\text{Cs}_2\text{AgBiBr}_6$ double perovskite. *Journal of Physical Chemistry C*, 122(45), 25940-25947.
- Keshavarz, M., Debroye, E., Ottesen, M., Martin, C., Zhang, H., Fron, E., Küchler, R., Steele, J. A., Bremholm, M., Van de Vondel, J., Wang, H. I., Bonn, M., Roeffaers, M. B. J., Wiedmann, S., & Hofkens, J. (2020). Tuning the structural and optoelectronic properties of $\text{Cs}_2\text{AgBiBr}_6$ double-perovskite single crystals through alkali-metal substitution. *Advanced Materials*, 32(40), 2001878.

- Kim, J., Park, J., Nam, S. W., Shin, M., Jun, S., Cho, Y. H., & Shin, B. (2020). Determining the chemical origin of the photoluminescence of cesium-bismuth-bromide perovskite nanocrystals and improving the luminescence via metal chloride additives. *ACS Applied Energy Materials*, 3(5), 4650-4657.
- Kittel, C. (2005). Wave diffraction and the reciprocal lattice. In *Introduction to solid state physics* (8th ed., pp. 25-45). John Wiley & Sons.
- Klime, J., Bowler, D. R., & Michaelides, A. (2011). Van der Waals density functionals applied to solids. *Physical Review B*, 83(19), 195131.
- Klimeš, J., Bowler, D. R., & Michaelides, A. (2010). Chemical accuracy for the van der Waals density functional. *Journal of Physics Condensed Matter*, 22(2), 022201.
- König, U., Angélica, R. S., Norberg, N., & Gobbo, L. (2012). Rapid X-ray diffraction (XRD) for grade control of bauxites. *ICSOBA Proceedings*, 19, 1-11.
- Krajewska, C. J., Kavanagh, S. R., Zhang, L., Kubicki, D. J., Dey, K., Gałkowski, K., Grey, C. P., Stranks, S. D., Walsh, A., Scanlon, D. O., & Palgrave, R. G. (2021). Enhanced visible light absorption in layered $\text{Cs}_3\text{Bi}_2\text{Br}_9$ through mixed-valence Sn(ii)/Sn(iv) doping. *Chemical Science*, 12(44), 14686–14699.
- Kshirsagar, A. S., & Nag, A. (2019). Synthesis and optical properties of colloidal $\text{Cs}_2\text{AgSb}_{1-x}\text{Bi}_x\text{Cl}_6$ double perovskite nanocrystals. *Journal of Chemical Physics*, 151(16), 161101.
- Kubicki, D. J., Saski, M., Macpherson, S., Gałkowski, K., Lewiński, J., Prochowicz, D., Titman, J. J., & Stranks, S. D. (2020). Halide mixing and phase segregation in $\text{Cs}_2\text{AgBiX}_6$ ($X = \text{Cl}$, Br , and I) double perovskites from cesium-133 solid-state NMR and optical spectroscopy. *Chemistry of Materials*, 32(19), 8129-8138.
- Kulbak, M., Gupta, S., Kedem, N., Levine, I., Bendikov, T., Hodes, G., & Cahen, D. (2016). Cesium enhances long-term stability of lead bromide perovskite-based solar cells. *Journal of Physical Chemistry Letters*, 7(1), 167-172.
- Kumar, A., Rawat, S. S., Swami, S. K., Singh, V. N., & Srivastava, R. (2019). Benzoyl halide as alternative precursor for synthesis of lead free double perovskite $\text{Cs}_3\text{Bi}_2\text{Br}_9$ nanocrystals. *Journal of Nanoscience and Nanotechnology*, 20(6), 38023808.
- Kumar, A., Swami, S. K., Rawat, S. S., Singh, V. N., Sinha, O. P., & Srivastava, R. (2021). Mixed bismuth-antimony-based double perovskite nanocrystals for solar cell application. *International Journal of Energy Research*, 45(11), 16769-16780.
- Kunal, P., & Toops, T. J. (2020). A review of microwave-assisted synthesis-based approaches to reduce Pd-content in catalysts. *Catalysts*, 10(9), 991.
- Lamba, R. S., Basera, P., Bhattacharya, S., & Sapra, S. (2019). Band gap engineering in $\text{Cs}_2(\text{Na}_x\text{Ag}_{1-x})\text{BiCl}_6$ double perovskite nanocrystals. *Journal of Physical Chemistry Letters*, 10(17), 5173-5181.

- Lamba, R. S., Basera, P., Singh, S., Bhattacharya, S., & Sapra, S. (2021). Lead-free alloyed double-perovskite nanocrystals of $\text{Cs}_2(\text{Na}_x\text{Ag}_{1-x})\text{BiBr}_6$ with tunable band gap. *Journal of Physical Chemistry C*, 125(3), 1954-1962.
- Lee, D., Kim, M. H., Woo, H. Y., Chae, J., Lee, D., Jeon, S., Oh, S. J., & Paik, T. (2020). Heating-up synthesis of cesium bismuth bromide perovskite nanocrystals with tailored composition, morphology, and optical properties. *RSC Advances*, 10(12), 7126–7133.
- Lee, J. W., Tan, S., Seok, S. Il, Yang, Y., & Park, N. G. (2022). Rethinking the A cation in halide perovskites. *Science*, 375(6583), eabj1186.
- Lee, K., Murray, É. D., Kong, L., Lundqvist, B. I., & Langreth, D. C. (2010). Higher-accuracy van der Waals density functional. *Physical Review*, 82(8), 081101.
- Leng, M., Chen, Z., Yang, Y., Li, Z., Zeng, K., Li, K., Niu, G., He, Y., Zhou, Q., & Tang, J. (2016a). Lead-Free, Blue Emitting Bismuth Halide Perovskite Quantum Dots. *Angewandte Chemie - International Edition*, 55(48), 15012-15016.
- Leng, M., Chen, Z., Yang, Y., Zeng, K., & Tang, J. (2016b). Synthesis and optical properties of lead-free methylamine bismuth halide perovskite quantum dots. In *Asia Communications and Photonics Conference* (pp. AS1I-5). Optica Publishing Group.
- Leng, M., Yang, Y., Zeng, K., Chen, Z., Tan, Z., Li, S., Li, J., Xu, B., Li, D., Hautzinger, M. P., Fu, Y., Zhai, T., Xu, L., Niu, G., Jin, S., & Tang, J. (2018). All-inorganic bismuth-based perovskite quantum dots with bright blue photoluminescence and excellent stability. *Advanced Functional Materials*, 28(1), 1704446.
- Leng, Y. (2010). X-ray diffraction method. In *Materials characterization: introduction to microscopic and spectroscopic methods* (pp. 52). John Wiley & Sons.
- Li, J., Duan, J., Yang, X., Duan, Y., Yang, P., & Tang, Q. (2021a). Review on recent progress of lead-free halide perovskites in optoelectronic applications. *Nano Energy*, 80, 105526.
- Li, Q., Song, T., Zhang, Y., Wang, Q., & Yang, Y. (2021b). Boosting photocatalytic activity and stability of lead-free $\text{Cs}_3\text{Bi}_2\text{Br}_9$ perovskite nanocrystals via in situ growth on monolayer 2D $\text{Ti}_3\text{C}_2\text{T}_x$ MXene for C-H bond oxidation. *ACS Applied Materials and Interfaces*, 13(23), 27323-27333.
- Li, Q., Wang, Y., Pan, W., Yang, W., Zou, B., Tang, J., & Quan, Z. (2017). High-pressure band-gap engineering in lead-free $\text{Cs}_2\text{AgBiBr}_6$ double perovskite. *Angewandte Chemie*, 56(50), 15969-15973.
- Li, Q., Yin, L., Chen, Z., Deng, K., Luo, S., Zou, B., Wang, Z., Tang, J., & Quan, Z. (2019a). High pressure structural and optical properties of two-dimensional hybrid halide perovskite $(\text{CH}_3\text{NH}_3)_3\text{Bi}_2\text{Br}_9$. *Inorganic Chemistry*, 58(2), 1621-1626.

- Li, W., Long, R., Tang, J., & Prezhdo, O. V. (2019b). Influence of defects on excited-state dynamics in lead halide perovskites: time-domain ab initio studies. *Journal of Physical Chemistry Letters*, 10(13), 3788-3804.
- Li, X., Du, X., Zhang, P., Hua, Y., Liu, L., Niu, G., Zhang, G., Tang, J., & Tao, X. (2021c). Lead-free halide perovskite $\text{Cs}_3\text{Bi}_2\text{Br}_9$ single crystals for high-performance X-ray detection. *Science China Materials*, 64(6), 1427-1436.
- Li, X., Mai, H., Cox, N., Lu, J., Wen, X., Chen, D., & Caruso, R. A. (2022). Sb-substituted $\text{Cs}_2\text{AgBiBr}_6/\text{g-C}_3\text{N}_4$ composite for photocatalytic C(sp³)-H bond activation in toluene. *Chemistry of Materials*, 35(8), 3105-3114.
- Li, Z., Kavanagh, S. R., Napari, M., Palgrave, R. G., Abdi-Jalebi, M., Andaji-Garmaroudi, Z., Davies, D. W., Laitinen, M., Julin, J., Isaacs, M. A., Friend, R. H., Scanlon, D. O., Walsh, A., & Hoye, R. L. Z. (2020). Bandgap lowering in mixed alloys of $\text{Cs}_2\text{Ag}(\text{Sb}_x\text{Bi}_{1-x})\text{Br}_6$ double perovskite thin films. *Journal of Materials Chemistry A*, 8(41), 21780-21788.
- Lian, L., Zhai, G., Cheng, F., Xia, Y., Zheng, M., Ke, J., Gao, M., Liu, H., Zhang, D., Li, L., Gao, J., Tang, J., & Zhang, J. (2018). Colloidal synthesis of lead-free all-inorganic cesium bismuth bromide perovskite nanoplatelets. *CrystEngComm*, 20(46), 7473-7478.
- Lindquist, K. P., Mack, S. A., Slavney, A. H., Leppert, L., Gold-Parker, A., Stebbins, J. F., Salleo, A., Toney, M. F., Neaton, J. B., & Karunadasa, H. I. (2019). Tuning the bandgap of $\text{Cs}_2\text{AgBiBr}_6$ through dilute tin alloying. *Chemical Science*, 10(45), 10620-10628.
- Liu, G., Zhang, Z., Wu, C., Zhang, Y., Li, X., Yu, W., Yao, G., Liu, S., Shi, J. jie, Liu, K., Chen, Z., Xiao, L., & Qu, B. (2022). Extending absorption of $\text{Cs}_2\text{AgBiBr}_6$ to near-infrared region (≈ 1350 nm) with intermediate band. *Advanced Functional Materials*, 32(12), 2109891.
- Liu, R., & Xu, K. (2020a). Solvent engineering for perovskite solar cells: a review. *Micro and Nano Letters*, 15(6), 349-353.
- Liu, T., Tang, W., Luong, S., & Fenwick, O. (2020b). High charge carrier mobility in solution processed one-dimensional lead halide perovskite single crystals and their application as photodetectors. *Nanoscale*, 12(17), 9688-9695.
- Liu, Y., Jing, Y., Zhao, J., Liu, Q., & Xia, Z. (2019a). Design optimization of lead-free perovskite $\text{Cs}_2\text{AgInCl}_6:\text{Bi}$ nanocrystals with 11.4% photoluminescence quantum yield. *Chemistry of Materials*, 31(9), 3333-3339.
- Liu, Y. L., Yang, C. L., Wang, M. S., Ma, X. G., & Yi, Y. G. (2019b). Theoretical insight into the optoelectronic properties of lead-free perovskite derivatives of $\text{Cs}_3\text{Sb}_2\text{X}_9$ (X = Cl, Br, I). *Journal of Materials Science*, 54(6), 4732-4741.
- Liu, Y., Zhang, L., Wang, M., Zhong, Y., Huang, M., Long, Y., & Zhu, H. (2019c). Bandgap-tunable double-perovskite thin films by solution processing. *Materials Today*, 28, 25-30.

- Liu, Z., Yang, H., Wang, J., Yuan, Y., Hills-Kimball, K., Cai, T., Wang, P., Tang, A., & Chen, O. (2021). Synthesis of lead-free $\text{Cs}_2\text{AgBiX}_6$ ($X = \text{Cl}, \text{Br}, \text{I}$) double perovskite nanoplatelets and their application in CO_2 photocatalytic reduction. *Nano Letters*, 24(4), 1620-1627.
- Locardi, F., Cirignano, M., Baranov, D., Dang, Z., Prato, M., Drago, F., Ferretti, M., Pinchetti, V., Fanciulli, M., Brovelli, S., De Trizio, L., & Manna, L. (2018). Colloidal synthesis of double perovskite $\text{Cs}_2\text{AgInCl}_6$ and Mn-doped $\text{Cs}_2\text{AgInCl}_6$ nanocrystals. *Journal of the American Chemical Society*, 140(40), 12989-12995.
- Locardi, F., Sartori, E., Buha, J., Zito, J., Prato, M., Pinchetti, V., Zaffalon, M. L., Ferretti, M., Brovelli, S., Infante, I., De Trizio, L., & Manna, L. (2019). Emissive Bi-doped double perovskite $\text{Cs}_2\text{Ag}_{1-x}\text{Na}_x\text{InCl}_6$ nanocrystals. *ACS Energy Letters*, 4(8), 1976-1982.
- Lou, Y., Fang, M., Chen, J., & Zhao, Y. (2018). Formation of highly luminescent cesium bismuth halide perovskite quantum dots tuned by anion exchange. *Chemical Communications*, 54(30), 3779-3782.
- Lu, C., Wright, M. W., Ma, X., Li, H., Itanze, D. S., Carter, J. A., Hewitt, C. A., Donati, G. L., Carroll, D. L., Lundin, P. M., & Geyer, S. M. (2019). Cesium oleate precursor preparation for lead halide perovskite nanocrystal synthesis: the influence of excess oleic acid on achieving solubility, conversion, and reproducibility. *Chemistry of Materials*, 31(1), 62-67.
- Lu, H., Krishna, A., Zakeeruddin, S. M., Grätzel, M., & Hagfeldt, A. (2020). Compositional and interface engineering of organic-inorganic lead halide perovskite solar cells. *iScience*, 23(8), 1-14.
- Lu, T., Ma, Z., Du, C., Fang, Y., Wu, H., Jiang, Y., Wang, L., Dai, L., Jia, H., Liu, W., & Chen, H. (2014). Temperature-dependent photoluminescence in light-emitting diodes. *Scientific Reports*, 4(1), 6131.
- Luo, T., & Wei, J. (2020). First principles study of electronic and optical properties of inorganic and lead-free perovskite: $\text{Cs}_3\text{Bi}_2\text{X}_9$ ($X: \text{Cl}, \text{Br}, \text{I}$). *Materials Chemistry and Physics*, 253, 123374.
- Lutterotti, L., Campstrini, R., Di Maggio, R., & Gialanella, S. (2000). Microstructural characterization of amorphous and nanocrystalline structures through diffraction methods. *Materials Science Forum*, 343, 657-664.
- Lv, C., Yang, X., Shi, Z., Wang, L., Sui, L., Li, Q., Qin, J., Liu, K., Zhang, Z., Li, X., Lou, Q., Yang, D., Zang, J., Liu, R., Liu, B., & Shan, C. X. (2020). Pressure-induced ultra-broad-band emission of a $\text{Cs}_2\text{AgBiBr}_6$ perovskite thin film. *Journal of Physical Chemistry C*, 124(2), 1732-1738.
- Lyu, C., Liu, C., Min, H., Shi, X., Jiang, R., Ao, Z., Zhang, X., Wang, C., Ma, H., & Wang, L. (2022). Rare earth Nd-doping lead-free double perovskite $\text{Cs}_2\text{AgBiBr}_6$ films with improved resistive memory performance. *Journal of Alloys and Compounds*, 913, 165300.

- Ma, Z. Z., Shi, Z. F., Wang, L. T., Zhang, F., Wu, D., Yang, D. W., Chen, X., Zhang, Y., Shan, C. X., & Li, X. J. (2020). Water-induced fluorescence enhancement of lead-free cesium bismuth halide quantum dots by 130% for stable white light-emitting devices. *Nanoscale*, 12(6), 3637-3645.
- Makuła, P., Pacia, M., & Macyk, W. (2018). How To Correctly Determine the band gap energy of modified semiconductor photocatalysts based on UV-Vis spectra. *Journal of Physical Chemistry Letters*, 9(23), 6814-6817.
- Mannino, G., Deretzis, I., Smecca, E., La Magna, A., Alberti, A., Ceratti, D., & Cahen, D. (2020). Temperature-dependent optical band gap in CsPbBr₃, MAPbBr₃, and FAPbBr₃ single crystals. *Journal of Physical Chemistry Letters*, 11(7), 2490-2496.
- Martín-García, B., Spirito, D., Biffi, G., Artyukhin, S., Francesco Bonaccorso, & Krahne, R. (2021). Phase transitions in low-dimensional layered double perovskites: the role of the organic moieties. *Journal of Physical Chemistry Letters*, 12(1), 280-286.
- McCall, K. M., Stoumpos, C. C., Kostina, S. S., Kanatzidis, M. G., & Wessels, B. W. (2017). Strong electron-phonon coupling and self-trapped excitons in the defect halide perovskites A₃M₂I₉ (A = Cs, Rb; M = Bi, Sb). *Chemistry of Materials*, 29(9), 4129-4145.
- McClure, E. T., Ball, M. R., Windl, W., & Woodward, P. M. (2016). Cs₂AgBiX₆ (X = Br, Cl): new visible light absorbing, lead-free halide perovskite semiconductors. *Chemistry of Materials*, 28(5), 1348-1354.
- Miao, Y., Ke, Y., Wang, N., Zou, W., Xu, M., Cao, Y., Sun, Y., Yang, R., Wang, Y., Tong, Y., Xu, W., Zhang, L., Li, R., Li, J., He, H., Jin, Y., Gao, F., Huang, W., & Wang, J. (2019). Stable and bright formamidinium-based perovskite light-emitting diodes with high energy conversion efficiency. *Nature Communications*, 10(1), 3624.
- Monkhorst, H. J., & Pack, J. D. (1976). Special points for Brillouin-zone integrations. *Physical Review B*, 13(12), 5188.
- Morgan, E. E., Mao, L., Teicher, S. M. L., Wu, G., & Seshadri, R. (2020). Tunable perovskite-derived bismuth halides: Cs₃Bi₂(Cl_{1-x}I_x)₉. *Inorganic Chemistry*, 59(6), 3387-3393.
- Mukhtar, M. W., Ramzan, M., Rashid, M., Hussain, A., Imran, M., Fahim, F., & Neffati, R. (2022). Ab-initio study of lead-free double perovskites Cs₂AgZBr₆ (Z = Bi, Sb) for solar cells and other renewable energy applications. *Journal of Solid State Chemistry*, 306, 122781.
- Nayak, J., Devi, C., & Vidyapeeth, L. (2016). Microwave assisted synthesis : a green chemistry approach. *International Research Journal of Pharmaceutical and Applied Sciences*, 3(5), 278–285.
- Nelson, R. D., Santra, K., Wang, Y., Hadi, A., Petrich, J. W., & Panthani, M. G. (2018). Synthesis and optical properties of ordered-vacancy perovskite cesium bismuth halide nanocrystals. *Chemical Communications*, 54(29), 3640-3643.

- Ning, W., Bao, J., Puttisong, Y., Moro, F., Kobera, L., Shimono, S., Wang, L., Ji, F., Cuartero, M., Kawaguchi, S., Abbrent, S., Ishibashi, H., de Marco, R., Bouianova, I. A., Crespo, G. A., Kubota, Y., Brus, J., Chung, D. Y., Sun, L., Chen, W. M., Kanatzidis, M. G., & Gao, F. (2020). Magnetizing lead-free halide double perovskites. *Science Advances*, 6(45), eabb5381.
- Ning, W., & Gao, F. (2019). Structural and functional diversity in lead-free halide perovskite materials. *Advanced Materials*, 31(22), 1900326.
- Otero-Martínez, C., Imran, M., Schrenker, N. J., Ye, J., Ji, K., Rao, A., Stranks, S. D., Hoye, R. L. Z., Bals, S., Manna, L., Pérez-Juste, J., & Polavarapu, L. (2022). Fast A-site cation cross exchange at room temperature: single-to double- and triple-cation halide perovskite nanocrystals. *Angewandte Chemie*, 134(34), e202205617.
- Ou, Y., Lu, Z., Lu, J., Zhong, X., Chen, P., Zhou, L., & Chen, T. (2022). Boosting the stability and efficiency of $\text{Cs}_2\text{AgBiBr}_6$ perovskite solar cells via Zn doping. *Optical Materials*, 129, 112452.
- Pahari, B., Chakraborty, S., Sengupta, B., Chaudhuri, S., Martin, W., Taylor, J., Henley, J., Davis, D., Biswas, P. K., Sharma, A. K., & Sengupta, P. K. (2013). Biophysical characterization of genistein in its natural carrier human hemoglobin using spectroscopic and computational approaches. *Food and Nutrition Sciences*, 4(8A), 83–92.
- Palummo, M., Berrios, E., Varsano, D., & Giorgi, G. (2020). Optical properties of lead-free double perovskites by ab initio excited-state methods. *ACS Energy Letters*, 5(2), 457–463.
- Pan, H., Xu, X., Liu, J., Li, X., Zhang, H., Huang, A., & Xiao, Z. (2021). Microwave-assisted synthesis of blue-emitting cesium bismuth bromine perovskite nanocrystals without polar solvent. *Journal of Alloys and Compounds*, 886, 161248.
- Pan, Q., Hu, H., Zou, Y., Chen, M., Wu, L., Yang, D., Yuan, X., Fan, J., Sun, B. & Zhang, Q. (2017). Microwave-assisted synthesis of high-quality “all-inorganic” CsPbX_3 ($X = \text{Cl}, \text{Br}, \text{I}$) perovskite nanocrystals and their application in light emitting diodes. *Journal of Materials Chemistry C*, 5(42), 10947–10954.
- Pan, W., Wu, H., Luo, J., Deng, Z., Ge, C., Chen, C., Jiang, X., Yin, W. J., Niu, G., Zhu, L., Yin, L., Zhou, Y., Xie, Q., Ke, X., Sui, M., & Tang, J. (2017). $\text{Cs}_2\text{AgBiBr}_6$ single-crystal X-ray detectors with a low detection limit. *Nature Photonics*, 11(11), 726–732.
- Pantaler, M., Diez-Cabanes, V., Queloz, V. I. E., Sutanto, A., Schouwink, P. A., Pastore, M., García-Benito, I., Nazeeruddin, M. K., Beljonne, D., Lupascu, D. C., Quarti, C., & Grancini, G. (2022). Revealing weak dimensional confinement effects in excitonic silver/bismuth double perovskites. *JACS Au*, 2(1), 136–149.

- Pantaler, M., Olthof, S., Meerholz, K., & Lupascu, D. C. (2019). Bismuth-antimony mixed double perovskites $\text{Cs}_2\text{AgBi}_{1-x}\text{Sb}_x\text{Br}_6$ in solar cells. *MRS Advances*, 4(64), 3545–3552.
- Pazoki, M., Johansson, M. B., Zhu, H., Broqvist, P., Edvinsson, T., Boschloo, G., & Johansson, E. M. J. (2016). Bismuth iodide perovskite materials for solar cell applications: electronic structure, optical transitions, and directional charge transport. *Journal of Physical Chemistry C*, 120(51), 29039–29046.
- Perdew, J. P., Burke, K., & Ernzerhof, M. (1996). Generalized gradient approximation made simple. *Physical Review Letters*, 77(18), 3865.
- Perdew, J. P., Ruzsinszky, A., Csonka, G. I., Vydrov, O. A., Scuseria, G. E., Constantin, L. A., Zhou, X., & Burke, K. (2008). Restoring the density-gradient expansion for exchange in solids and surfaces. *Physical Review Letters*, 100(13), 136406.
- Pistor, P., Meyns, M., Guc, M., Wang, H. C., Marques, M. A. L., Alcobé, X., Cabot, A., & Izquierdo-Roca, V. (2020). Advanced raman spectroscopy of $\text{Cs}_2\text{AgBiBr}_6$ double perovskites and identification of $\text{Cs}_3\text{Bi}_2\text{Br}_9$ secondary phases. *Scripta Materialia*, 184, 24-29.
- Prime, R. B., Bair, H. E., Vyazovkin, S., Gallagher, P. K., & Riga, A. (2008). Thermogravimetric analysis (TGA). In *Thermal Analysis of Polymers: Fundamentals and Applications* (pp. 241–317). John Wiley & Sons.
- Puttisong, Y., Moro, F., Chen, S. L., Höjer, P., Ning, W., Gao, F., Buyanova, I. A., & Chen, W. M. (2020). Effect of crystal symmetry on the spin states of Fe^{3+} and vibration modes in lead-free double-perovskite $\text{Cs}_2\text{AgBi(Fe)Br}_6$. *Journal of Physical Chemistry Letters*, 11(12), 4873-4878.
- Quan, L. N., Yang, P., & Guo, P. (2022). Octahedral distortion and excitonic behavior of $\text{Cs}_3\text{Bi}_2\text{Br}_9$ halide perovskite at low temperature. *Journal of Physical Chemistry C*, 127(7), 3523-3531.
- Radhakrishnan, R. (2020). Optoelectronic properties of all-Inorganic lead-free halide double perovskites $(\text{Rb}_x\text{Cs}_{1-x})_2\text{AgBiBr}_6$ for solar cell applications. *Indian Journal of Chemistry -Section A*, 59(9), 1298-1304.
- Reyes-Francis, E., Echeverría-Arrondo, C., Esparza, D., López-Luke, T., Soto-Montero, T., Morales-Masis, M., Turren-Cruz, S., Mora-Seró, I. & Julián-López, B. (2024). Microwave-mediated synthesis of lead-free cesium titanium bromide double perovskite: a sustainable approach. *Chemistry of Materials*, 36(3), 1728-1836.
- Rieger, S., Bohn, B. J., Döblinger, M., Richter, A. F., Tong, Y., Wang, K., Müller-Buschbaum, P., Polavarapu, L., Leppert, L., Stolarczyk, J. K., & Feldmann, J. (2019). Excitons and narrow bands determine the optical properties of cesium bismuth halides. *Physical Review B*, 100(20), 201404.

- Rodkey, N., Kaal, S., Sebastia-Luna, P., Birkhölzer, Y. A., Ledinsky, M., Palazon, F., Bolink, H. J., & Morales-Masis, M. (2021). Pulsed laser deposition of $\text{Cs}_2\text{AgBiBr}_6$: from mechanochemically synthesized powders to dry, single-step deposition. *Chemistry of Materials*, 33(18), 7417-7422.
- Romani, L., Speltini, A., Dibenedetto, C. N., Listorti, A., Ambrosio, F., Mosconi, E., Simbula, A., Saba, M., Profumo, A., Quadrelli, P., De Angelis, F., & Malavasi, L. (2021). Experimental strategy and mechanistic view to boost the photocatalytic activity of $\text{Cs}_3\text{Bi}_2\text{Br}_9$ lead-free perovskite derivative by g-C₃N₄ composite engineering. *Advanced Functional Materials*, 31(46), 2104428.
- Roy, M., Ghorui, S., Bhawna, Kangsabanik, J., Yadav, R., Alam, A., & Aslam, M. (2020). Enhanced visible light absorption in layered $\text{Cs}_3\text{Bi}_2\text{Br}_9$ halide perovskites: heterovalent Pb²⁺ substitution-induced defect band formation. *The Journal of Physical Chemistry C*, 124(36), 19484-19491.
- Samanta, D., Saha, P., Ghosh, B., Chaudhary, S., Bhattacharyya, S., Chatterjee, S., & Mukherjee, G. (2020). Pressure induced emergence of visible luminescence in $\text{Cs}_3\text{Bi}_2\text{Br}_9$: effect of structural distortion in optical behaviour. *Journal of Physical Chemistry C*, 125, 3432-3440.
- Sani, F., Shafie, S., Lim, H. N., & Musa, A. O. (2018). Advancement on lead-free organic-inorganic halide perovskite solar cells: A review. *Materials*, 11(6), 1008.
- Schade, L., Mahesh, S., Volonakis, G., Zacharias, M., Wenger, B., Schmidt, F., Kesava, S. V., Prabhakaran, D., Abdi-Jalebi, M., Lenz, M., Giustino, F., Longo, G., Radaelli, P. G., & Snaith, H. J. (2021). Crystallographic, optical, and electronic properties of the $\text{Cs}_2\text{AgBi}_{1-x}\text{In}_x\text{Br}_6$ double perovskite: understanding the fundamental photovoltaic efficiency challenges. *ACS Energy Letters*, 6(3), 1073-1081.
- Schade, L., Wright, A. D., Johnson, R. D., Dollmann, M., Wenger, B., Nayak, P. K., Prabhakaran, D., Herz, L. M., Nicholas, R., Snaith, H. J., & Radaelli, P. G. (2019). Structural and optical properties of $\text{Cs}_2\text{AgBiBr}_6$ double perovskite. *ACS Energy Letters*, 4(1), 299-305.
- Schmitz, A., Leander Schaberg, L., Sirotinskaya, S., Pantaler, M., Lupascu, D. C., Benson, N., & Bacher, G. (2020). Fine structure of the optical absorption resonance in $\text{Cs}_2\text{AgBiBr}_6$ double perovskite thin films. *ACS Energy Letters*, 5(2), 559-565.
- Schmitz, F., Guo, K., Horn, J., Sorrentino, R., Conforto, G., Lamberti, F., Brescia, R., Drago, F., Prato, M., He, Z., Giovanella, U., Cacialli, F., Schlettwein, D., Meggiolaro, D., & Gatti, T. (2020). Lanthanide-induced photoluminescence in lead-free $\text{Cs}_2\text{AgBiBr}_6$ bulk perovskite: insights from optical and theoretical investigations. *Journal of Physical Chemistry Letters*, 11(20), 8893-8900.
- Schmitz, F., Horn, J., Dengo, N., Sedykh, A. E., Becker, J., Maiworm, E., Bélteky, P., Kukovecz, Á., Gross, S., Lamberti, F., Müller-Buschbaum, K., Schlettwein, D., Meggiolaro, D., Righetto, M., & Gatti, T. (2021). Large cation engineering in two-dimensional silver–bismuth bromide double perovskites. *Chemistry of Materials*, 33(12), 4688-4700.

- Sebastiá-Luna, P., Calbo, J., Albiach-Sebastián, N., Sessolo, M., Palazón, F., Ortí, E., & Bolink, H. J. (2021). Tuning the optical absorption of Sn-, Ge-, and Zn-substituted $\text{Cs}_2\text{AgBiBr}_6$ double perovskites: structural and electronic effects. *Chemistry of Materials*, 33(20), 8028-8035.
- Shadabroo, M. S., Abdizadeh, H., & Golobostanfar, M. R. (2021). Elpasolite structures based on A_2AgBiX_6 (A : MA, Cs, X: I, Br): Application in double perovskite solar cells. *Materials Science in Semiconductor Processing*, 125, 105639.
- Shamsi, J., Urban, A. S., Imran, M., De Trizio, L., & Manna, L. (2019). Metal halide perovskite nanocrystals: synthesis, post-synthesis modifications, and their optical properties. *Chemical Reviews*, 119(5), 3296-3348.
- Shao, Q., Yan, J., Gong, W., Li, Y., Gao, F., Wang, B., & Li, L. (2022). Dopant-compensated $\text{Cs}_2\text{AgBiBr}_{6-x}\text{Cl}_x$ single crystals for photo-imaging and X-ray detection. *Journal of Materials Chemistry C*, 10(48), 18366-18374.
- Shen, Y., Yin, J., Cai, B., Wang, Z., Dong, Y., Xu, X., & Zeng, H. (2020). Lead-free, stable, high-efficiency (52%) blue luminescent $\text{FA}_3\text{Bi}_2\text{Br}_9$ perovskite quantum dots. *Nanoscale Horizons*, 5(3), 580-585.
- Shi, M., Li, G., Tian, W., Jin, S., Tao, X., Jiang, Y., Pidko, E. A., Li, R., & Li, C. (2020). Understanding the effect of crystalline structural transformation for lead-free inorganic halide perovskites. *Advanced Materials*, 32(31), 2002137.
- Shi, M., Yang, B., Liu, S., Zhang, R., Han, K., Li, C., & Li, R. (2023). Tuning exciton recombination pathways in inorganic bismuth-based perovskite for broadband emission. *Energy Material Advances*, 2022, 1-11.
- Shi, M., Zhou, H., Tian, W., Yang, B., Yang, S., Han, K., Li, R., & Li, C. (2021). Lead-free B-site bimetallic perovskite photocatalyst for efficient benzylic C–H bond activation. *Cell Reports Physical Science*, 2(12), 100656.
- Sikarwar, P., Siwach, P., Phani Chandra, N. V., Antharjanam, S., & Chandiran, A. K. (2023). Dimensional reduction of $\text{Cs}_2\text{AgBiBr}_6$ using alkyl ammonium cations $\text{CH}_3(\text{CH}_2)_n\text{NH}^{3+}$ ($n = 1, 2, 3$, and 6) of varying chain lengths and their role in structural and optoelectronic properties. *Inorganic Chemistry*, 62(14), 5836-5844.
- Sirtl, M. T., Armer, M., Reb, L. K., Hooijer, R., Dörflinger, P., Scheel, M. A., Tvingstedt, K., Rieder, P., Glück, N., Pandit, P., Roth, S. V., Müller-Buschbaum, P., Dyakonov, V., & Bein, T. (2020). Optoelectronic properties of $\text{Cs}_2\text{AgBiBr}_6$ thin films: the influence of precursor stoichiometry. *ACS Applied Energy Materials*, 3(12), 11597-11609.
- Slavney, A. H., Hu, T., Lindenberg, A. M., & Karunadasa, H. I. (2016). A bismuth-halide double perovskite with long carrier recombination lifetime for photovoltaic applications. *Journal of the American Chemical Society*, 138(7), 2138-2141.

- Slavney, A. H., Leppert, L., Bartesaghi, D., Gold-Parker, A., Toney, M. F., Savenije, T. J., Neaton, J. B., & Karunadasa, H. I. (2017). Defect-induced band-edge reconstruction of a bismuth-halide double perovskite for visible-light absorption. *Journal of the American Chemical Society*, 139(14), 5015–5018.
- Solis, O. E., Fernández-Saiz, C., Rivas, J. M., Esparza, D., Turren-Cruz, S. H., Julián-López, B., Boix, P. P. & Mora-Seró, I. (2023). α -FAPbI₃ powder presynthesized by microwave irradiation for photovoltaic applications. *Electrochimica Acta*, 439, 141701.
- Soosaimanickam, A., Rodríguez-Cantó, P. J., Martínez-Pastor, J. P., & Abargues, R. (2020). Recent advances in synthesis, surface chemistry of cesium lead-free halide perovskite nanocrystals and their potential applications. *Nanostructured, Functional, and Flexible Materials for Energy Conversion and Storage Systems*, 157–228.
- Steele, J. A., Puech, P., Keshavarz, M., Yang, R., Banerjee, S., Debroye, E., Kim, C. W., Yuan, H., Heo, N. H., Vanacken, J., Walsh, A., Hofkens, J., & Roeffaers, M. B. J. (2018). Giant electron-phonon coupling and deep conduction band resonance in metal halide double perovskite. *ACS Nano*, 12(8), 8081–8090.
- Su, J., Huang, Y. qiang, Chen, H., & Huang, J. (2020a). Solution growth and performance study of Cs₂AgBiBr₆ single crystal. *Crystal Research and Technology*, 55(3), 1900222.
- Su, J., Mou, T., Wen, J., & Wang, B. (2020b). First-principles study on the structure, electronic, and optical properties of Cs₂AgBiBr_{6-x}Cl_x mixed-halide double perovskites. *Journal of Physical Chemistry C*, 124(9), 5371–5377.
- Sugathan, V., Kangsabanik, J., Alam, A., & Yella, A. (2022). Lead-free potassium alloyed Cs₂AgBiBr₆: tunable optoelectronic properties and carrier-lattice interaction. *Energy and Fuels*, 36(18), 11100–11107.
- Sun, C., Luo, F., Ruan, L., Tong, J., Yan, L., Zheng, Y., Han, X., Zhang, Y., & Zhang, X. (2021). Enhanced memristive performance of double perovskite Cs₂AgBiBr_{6-x}Cl_x devices by chloride doping. *ChemPlusChem*, 86(11), 1530–1536.
- Sun, K., Hu, Z., Shen, B., Lu, C., Yang, C., Gao, C., Zhang, J., & Zhu, Y. (2018). Balancing transformation and dissolution-crystallization for pure phase CH₃NH₃PbI₃ growth and its effect on photovoltaic performance in planar-structure perovskite solar cells. *Solar Energy Materials and Solar Cells*, 185, 464–470.
- Tailor, N. K., & Satapathi, S. (2020). Structural disorder and spin dynamics study in millimeter-sized all-inorganic lead-free cesium bismuth halide perovskite single crystals. *ACS Applied Energy Materials*, 3(12), 11732–11740.
- Tang, H., Xu, Y., Hu, X., Hu, Q., Chen, T., Jiang, W., Wang, L., & Jiang, W. (2021a). Lead-free halide double perovskite nanocrystals for light-emitting applications: strategies for boosting efficiency and stability. *Advanced Science*, 8(7), 2004118.

- Tang, Y., Gomez, L., Van Der Laan, M., Timmerman, D., Sebastian, V., Huang, C. C., Gregorkiewicz, T., & Schall, P. (2021b). Room temperature synthesis and characterization of novel lead-free double perovskite nanocrystals with a stable and broadband emission. *Journal of Materials Chemistry C*, 9(1), 158-163.
- Tang, Y., Liang, M., Chang, B., Sun, H., Zheng, K., Pullerits, T., & Chi, Q. (2019). Lead-free double halide perovskite Cs_3BiBr_6 with well-defined crystal structure and high thermal stability for optoelectronics. *Journal of Materials Chemistry C*, 7(11), 3369-3374.
- Thesika, K., & Vadivel Murugan, A. (2020). Microwave-enhanced chemistry at solid–liquid interfaces: synthesis of all-inorganic CsPbX_3 nanocrystals and unveiling the anion-induced evolution of structural and optical properties. *Inorganic chemistry*, 59(9), 6161-6175.
- Toby, B. H. (2006). R factors in Rietveld analysis: how good is good enough? *Powder Diffraction*, 21(1), 67–70.
- Tran, M. N., Cleveland, I. J., & Aydil, E. S. (2020). Resolving the discrepancies in the reported optical absorption of low-dimensional non-toxic perovskites, $\text{Cs}_3\text{Bi}_2\text{Br}_9$ and Cs_3BiBr_6 . *Journal of Materials Chemistry C*, 8(30), 10456-10463.
- Tran, M. N., Cleveland, I. J., & Aydil, E. S. (2022a). Reactive physical vapor deposition of Yb-doped lead-free double perovskite $\text{Cs}_2\text{AgBiBr}_6$ with 95% photoluminescence quantum yield. *ACS Applied Electronic Materials*, 4(9), 4588-4594.
- Tran, M. N., Cleveland, I. J., Geniesse, J. R., & Aydil, E. S. (2022b). High photoluminescence quantum yield near-infrared emission from a lead-free ytterbium-doped double perovskite. *Materials Horizons*, 9(8), 2191-2197.
- Tripathi, M., Saha, A., & Singh, S. (2019). Structural, elastic, electronic and optical properties of lead-free halide double perovskite $\text{Cs}_2\text{AgBiX}_6$ (X=Cl, Br, and I). *Materials Research Express*, 6(11), 115517.
- Turren-Cruz, S. H., Hagfeldt, A., & Saliba, M. (2018). Methylammonium-free, high-performance, and stable perovskite solar cells on a planar architecture. *Science*, 362(6413), 449-453.
- Umari, P., Mosconi, E., & De Angelis, F. (2018). Infrared dielectric screening determines the low exciton binding energy of metal-halide perovskites. *Journal of Physical Chemistry Letters*, 9(3), 620-627.
- Ünlü, F., Jung, E., Haddad, J., Kulkarni, A., Öz, S., Choi, H., Fischer, T., Chakraborty, S., Kirchartz, T., & Mathur, S. (2020). Understanding the interplay of stability and efficiency in A-site engineered lead halide perovskites. *APL Materials*, 8(7), 1-15.

- Vasilopoulou, M., Fakharuddin, A., Coutsolelos, A. G., Falaras, P., Argitis, P., Yusoff, A. R. B. M., & Nazeeruddin, M. K. (2020). Molecular materials as interfacial layers and additives in perovskite solar cells. *Chemical Society Reviews*, 49(13), 4496-4526.
- Vigil, J. A., Hazarika, A., Luther, J. M., & Toney, M. F. (2020). $\text{FA}_x\text{Cs}_{1-x}\text{PbI}_3$ nanocrystals: tuning crystal symmetry by A-site cation composition. *ACS Energy Letters*, 5(8), 2475-2482.
- Wang, C., Ding, Y., Liu, B., Weng, B., Hofkens, J., & Roeffaers, M. B. J. (2023). Crystal structure engineering of metal halide perovskites for photocatalytic organic synthesis. *Chemical Communications*, 59(21), 3122-3125.
- Wang, T., Tong, Y., Chen, Y., Fang, Z., Qi, H., Chen, Y., Zhang, Y., Wang, H., Wang, K., & Wang, H. (2022). Replacing cesium with formamidinium cation in colloidal perovskite nanoplatelets: synthetic alloying and post-synthetic cation exchange towards efficient blue emission. *Journal of Luminescence*, 251, 119210.
- Wang, X., Bi, G., Ali, N., Chen, Y., & Wu, H. (2021a). Theoretical study of the strain influence on lead-free bismuth-based halide perovskites. *Journal of Materials Science*, 56, 11377-11385.
- Wang, Y., Dai, Y., & Tüysüz, H. (2021b). Preparation and properties of polystyrene nanospheres incorporated $\text{Cs}_3\text{Bi}_2\text{Br}_9$ halide perovskite disks. *European Journal of Inorganic Chemistry*, 2021(27), 2712-2717.
- Wasly, H. (2018). X-ray analysis for determination the crystallite size and lattice strain in ZnO nanoparticles. *Journal of Al-Azhar University Engineering Sector*, 13(49), 1312-1320.
- Wei, F., Deng, Z., Sun, S., Zhang, F., Evans, D. M., Kieslich, G., Tominaka, S., Carpenter, M. A., Zhang, J., Bristowe, P. D., & Cheetham, A. K. (2017). Synthesis and properties of a lead-free hybrid double perovskite: $(\text{CH}_3\text{NH}_3)_2\text{AgBiBr}_6$. *Chemistry of Materials*, 29(3), 1089-1094.
- Wheatley, R. A., Rojas, S., Oppolzer, C., Joshi, T., Borisov, P., Lederman, D., & Cabrera, A. L. (2017). Comparative study of the structural and optical properties of epitaxial CuFeO_2 and $\text{CuFe}_{1-x}\text{Ga}_x\text{O}_2$ delafossite thin films grown by pulsed laser deposition methods. *Thin Solid Films*, 626, 110-116.
- Wojtaś, M., Bator, G., & Baran, J. (2003). Vibrational study of structural phase transitions in $[(\text{CH}_3)_2\text{NH}_2]_3[\text{Bi}_2\text{Cl}_9]$ and $[(\text{CH}_3)_2\text{NH}_2]_3[\text{As}_2\text{Cl}_9]$ crystals. *Vibrational Spectroscopy*, 33(1), 143–152.
- Wright, A. D., Buizza, L. R. V., Savill, K. J., Longo, G., Snaith, H. J., Johnston, M. B., & Herz, L. M. (2021). Ultrafast excited-state localization in $\text{Cs}_2\text{AgBiBr}_6$ double perovskite. *Journal of Physical Chemistry Letters*, 12(13), 3352-3360.
- Wu, C., Zhang, Q., Liu, Y., Luo, W., Guo, X., Huang, Z., Ting, H., Sun, W., Zhong, X., Wei, S., Wang, S., Chen, Z., & Xiao, L. (2018). The dawn of lead-free perovskite solar cell: highly stable double perovskite $\text{Cs}_2\text{AgBiBr}_6$ film. *Advanced Science*, 5(3), 1700759.

- Wu, D., Tao, Y., Huang, Y., Huo, B., Zhao, X., Yang, J., Jiang, X., Huang, Q., Dong, F., & Tang, X. (2021a). High visible-light photocatalytic performance of stable lead-free $\text{Cs}_2\text{AgBiBr}_6$ double perovskite nanocrystals. *Journal of Catalysis*, 397, 27-35.
- Wu, H., Erbing, A., Johansson, M. B., Wang, J., Kamal, C., Odelius, M., & Johansson, E. M. J. (2021b). Mixed-halide double perovskite $\text{Cs}_2\text{AgBiX}_6$ (X=Br, I) with tunable optical properties via anion exchange. *ChemSusChem*, 14(20), 4507-4515.
- Wu, H., Liu, W., Ma, W., Liang, T., Liu, X., & Fan, J. (2022a). Special roles of two-dimensional octahedral frameworks in photodynamics of $\text{Cs}_3\text{Bi}_2\text{Br}_9$ nanoplatelets: electron and lattice-wave localization. *Applied Physics Letters*, 121(18), 181902.
- Wu, H., Wang, Y., Liu, A., Wang, J., Kim, B. J., Liu, Y., Fang, Y., Zhang, X., Boschloo, G., & Johansson, E. M. J. (2022b). Methylammonium bromide assisted crystallization for enhanced lead-free double perovskite photovoltaic performance. *Advanced Functional Materials*, 32(14), 2109402.
- Wu, Z., Kong Pang, W., Chen, L., Johannessen, B., & Guo, Z. (2021c). In situ synchrotron X-ray absorption spectroscopy studies of anode materials for rechargeable batteries. *Batteries and Supercaps*, 4(10), 1547-1566.
- Xiang, G., Wu, Y., Zhang, M., Cheng, C., Leng, J., & Ma, H. (2021). Dimension-dependent bandgap narrowing and metallization in lead-free halide perovskite $\text{Cs}_3\text{Bi}_2\text{X}_9$ (X = I, Br, and Cl) under high pressure. *Nanomaterials*, 11(10), 2712.
- Xiao, Z., Meng, W., Wang, J., & Yan, Y. (2016). Thermodynamic stability and defect chemistry of bismuth-based lead-free double perovskites. *ChemSusChem*, 9(18), 2628-2633.
- Xu, H., Liang, H., Zheng, J., Ning, G., Wang, L., Zeng, J., Zhao, H., & Li, C.-P. (2021). Ultrahigh stable lead halide perovskite nanocrystals as bright fluorescent label for the visualization of latent fingerprints. *Nanotechnology*, 32(37), 375601.
- Xu, J., Yu, S., Shang, X., & Chen, X. (2023). Temperature dependence of bandgap in lead-halide perovskites with corner-sharing octahedra. *Advanced Photonics Research*, 4(1), 2200193.
- Yan, G., Jiang, B., Xiao, Y., Zhao, C., Yuan, Y., & Liang, Z. (2022). Alkali metal ions induced high-quality all-inorganic $\text{Cs}_2\text{AgBiBr}_6$ perovskite films for flexible self-powered photodetectors. *Applied Surface Science*, 579, 152198.
- Yang, B., Chen, J., Hong, F., Mao, X., Zheng, K., Yang, S., Li, Y., Pullerits, T., Deng, W., & Han, K. (2017). Lead-free, air-stable all-Inorganic cesium bismuth halide perovskite nanocrystals. *Angewandte Chemie*, 56(41), 12471-12475.
- Yang, B., Chen, J., Yang, S., Hong, F., Sun, L., Han, P., Pullerits, T., Deng, W., & Han, K. (2018a). Lead-free silver-bismuth halide double perovskite nanocrystals. *Angewandte Chemie*, 130(19), 5457-5461.

- Yang, B., Hong, F., Chen, J., Tang, Y., Yang, L., Sang, Y., Xia, X., Guo, J., He, H., Yang, S., Deng, W., & Han, K. (2019). Colloidal synthesis and charge-carrier dynamics of $\text{Cs}_2\text{AgSb}_{1-y}\text{Bi}_y\text{X}_6$ ($\text{X}: \text{Br}, \text{Cl}; 0 \leq y \leq 1$) double perovskite nanocrystals. *Angewandte Chemie*, 131(8), 2300-2305.
- Yang, B., Mao, X., Hong, F., Meng, W., Tang, Y., Xia, X., Yang, S., Deng, W., & Han, K. (2018b). Lead-free direct band gap double-perovskite nanocrystals with bright dual-color emission. *Journal of the American Chemical Society*, 140(49), 17001-17006.
- Yang, J., Zhang, P., & Wei, S. H. (2018c). Band structure engineering of $\text{Cs}_2\text{AgBiBr}_6$ perovskite through order-disordered transition: a first-principle study. *Journal of Physical Chemistry Letters*, 9(1), 31-35.
- Yang, Z., Chueh, C. C., Liang, P. W., Crump, M., Lin, F., Zhu, Z., & Jen, A. K. Y. (2016). Effects of formamidinium and bromide ion substitution in methylammonium lead triiodide toward high-performance perovskite solar cells. *Nano Energy*, 22, 328-337.
- Yin, R., Yu, G., Cong, W. Y., Guan, C. B., Li, J., & Lu, Y. B. (2020). Modulation effect generated by A cations in hybrid $\text{A}_2\text{BB}'\text{X}_6$ double halogen perovskite materials. *ACS Applied Materials and Interfaces*, 12(40), 44789-44804.
- Yoon, S., Fett, B., Frebel, A., Kroisl, S., Herbig, B., Widenmeyer, M., Balke, B., Sextl, G., Mandel, K., & Weidenkaff, A. (2022). Sb-substituted $\text{Cs}_2\text{AgBiBr}_6$ —as much as it could be? —influence of synthesis methods on Sb-substitution level in $\text{Cs}_2\text{AgBiBr}_6$. *Energy Technology*, 10(8), 2200197.
- Yu, B. Bin, Liao, M., Yang, J., Chen, W., Zhu, Y., Zhang, X., Duan, T., Yao, W., Wei, S. H., & He, Z. (2019). Alloy-induced phase transition and enhanced photovoltaic performance: the case of $\text{Cs}_3\text{Bi}_2\text{I}_{9-x}\text{Br}_x$ perovskite solar cells. *Journal of Materials Chemistry A*, 7(15), 8818–8825.
- Zavitsas, A. A. (2015). Factors affecting the relation between stretching frequencies and bond lengths. Diatomic and polyatomic species without adjustable fitting parameters. *Spectrochimica Acta - Part A: Molecular and Biomolecular Spectroscopy*, 151, 553-565.
- Zelewski, S. J., Urban, J. M., Surrente, A., Maude, D. K., Kuc, A., Schade, L., Johnson, R. D., Dollmann, M., Nayak, P. K., Snaith, H. J., Radaelli, P., Kudrawiec, R., Nicholas, R. J., Plochocka, P., & Baranowski, M. (2019). Revealing the nature of photoluminescence emission in the metal-halide double perovskite $\text{Cs}_2\text{AgBiBr}_6$. *Journal of Materials Chemistry C*, 7(27), 8350-8356.
- Zhang, C.-R., Chen, H., Liu, Z.-J., Zhang, M.-L., Wang, W., Wu, Y.-Z., & Chen, H.-S. (2022a). Formamidinium dopant effects on double perovskite $\text{Cs}_2\text{AgBiBr}_6$. *International Journal of Quantum Chemistry*, 122(4), e26846.
- Zhang, J., Yang, Y., Deng, H., Farooq, U., Yang, X., Khan, J., Tang, J., & Song, H. (2017a). High Quantum Yield Blue Emission from Lead-Free Inorganic Antimony Halide Perovskite Colloidal Quantum Dots. *ACS Nano*, 11(9), 9294-9302.

- Zhang, P., Yang, J., & Wei, S. H. (2018). Manipulation of cation combinations and configurations of halide double perovskites for solar cell absorbers. *Journal of Materials Chemistry A*, 6(4), 1809-1815.
- Zhang, W., Zhu, H., Pan, S., Li, H., Zhang, J., Gong, Z., Zhang, Y., & Pan, J. (2020). Growth and properties of centimeter-sized lead free all inorganic perovskite $\text{Cs}_2\text{AgBiBr}_6$ crystal by additive CH_3COONa . *Journal of Crystal Growth*, 532, 125440.
- Zhang, Y., Aly, O. F., De Gorostiza, A., Shuga Aldeen, T., Segapeli, A. J., & Korgel, B. A. (2023). Cesium methylammonium lead iodide ($\text{Cs}_x\text{MA}_{1-x}\text{PbI}_3$) nanocrystals with wide range cation composition tuning and enhanced thermal stability of the perovskite phase. *Angewandte Chemie*, 62(31), e202306005.
- Zhang, Y., Shah, T., Deepak, F. L., & Korgel, B. A. (2019a). Surface science and colloidal stability of double-perovskite $\text{Cs}_2\text{AgBiBr}_6$ nanocrystals and their superlattices. *Chemistry of Materials*, 31(19), 7962-7969.
- Zhang, Y., Song, Y., Lu, Y., Zhang, Z., Wang, Y., Yang, Y., Dong, Q., Yu, Y., Qin, P., & Huang, F. (2022b). Thermochromic $\text{Cs}_2\text{AgBiBr}_6$ single crystal with decreased band gap through order-disorder transition. *Small*, 18(24), 2201943.
- Zhang, Y., Yin, J., Parida, M. R., Ahmed, G. H., Pan, J., Bakr, O. M., Brédas, J. L., & Mohammed, O. F. (2017b). Direct-indirect nature of the bandgap in lead-free perovskite nanocrystals. *Journal of Physical Chemistry Letters*, 8(14), 3173-3177.
- Zhang, Z., Liu, G., Guo, W., Li, X., Zhang, Y., Wu, C., Qu, B., Shi, J., Chen, Z., & Xiao, L. (2022c). Black single crystals of lead-free perovskite $\text{Cs}_2\text{Ag}(\text{Bi}: \text{Ru})\text{Br}_6$ with an intermediate band. *Materials Advances*, 3(12), 4932-4937.
- Zhang, Z., Wu, C., Wang, D., Liu, G., Zhang, Q., Luo, W., Qi, X., Guo, X., Zhang, Y., Lao, Y., Qu, B., Xiao, L., & Chen, Z. (2019b). Improvement of $\text{Cs}_2\text{AgBiBr}_6$ double perovskite solar cell by rubidium doping. *Organic Electronics*, 74, 204-210.
- Zheng, K., Zhu, Q., Abdellah, M., Messing, M. E., Zhang, W., Generalov, A., Niu, Y., Ribaud, L., Canton, S. E., & Pullerits, T. (2015). Exciton binding energy and the nature of emissive states in organometal halide perovskites. *Journal of Physical Chemistry Letters*, 6(15), 2926-2975.
- Zhou, L., Xu, Y. F., Chen, B. X., Kuang, D. Bin, & Su, C. Y. (2018). Synthesis and photocatalytic application of stable lead-free $\text{Cs}_2\text{AgBiBr}_6$ perovskite nanocrystals. *Small*, 14(911), 1703762.
- Zhou, Y. Q., Liu, J. B., & Liu, B. X. (2021). Electronic structure and stability of the (001) surface of halide double perovskite $\text{Cs}_2\text{AgBiBr}_6$. *Applied Surface Science*, 570, 151223.